

2000

The use of Long-Lived Tracer Observations to Examine Transport Characteristics in the Lower Stratosphere

Gretchen Scott Lingenfelter
College of William & Mary - Arts & Sciences

Follow this and additional works at: <https://scholarworks.wm.edu/etd>

 Part of the [Atmospheric Sciences Commons](#)

Recommended Citation

Lingenfelter, Gretchen Scott, "The use of Long-Lived Tracer Observations to Examine Transport Characteristics in the Lower Stratosphere" (2000). *Dissertations, Theses, and Masters Projects*. Paper 1539626247.

<https://dx.doi.org/doi:10.21220/s2-sb5j-pe03>

This Thesis is brought to you for free and open access by the Theses, Dissertations, & Master Projects at W&M ScholarWorks. It has been accepted for inclusion in Dissertations, Theses, and Masters Projects by an authorized administrator of W&M ScholarWorks. For more information, please contact scholarworks@wm.edu.

THE USE OF LONG-LIVED TRACER OBSERVATIONS TO EXAMINE
TRANSPORT CHARACTERISTICS IN THE LOWER STRATOSPHERE

A Thesis

Presented to

The Faculty of the Department of Applied Science

The College of William and Mary in Virginia

In Partial Fulfillment

Of the Requirements for the Degree of

Master of Arts

by

Gretchen Scott Lingenfelter

2000

APPROVAL SHEET

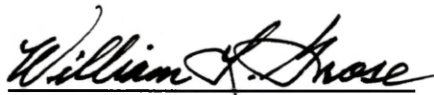
This thesis is submitted in partial fulfillment of
the requirements for the degree of

Master of Arts



Gretchen Lingenfelter

Approved, May 2000



William Grose



Mark Hinders



Joel Levine



Gerald Johnson
Department of Geology

TABLE OF CONTENTS

	Page
ACKNOWLEDGEMENTS	v
LIST OF FIGURES	vi
ABSTRACT	ix
CHAPTER I. INTRODUCTION	2
CHAPTER II. DATA DESCRIPTION	12
2.1 Satellite Data	13
2.1.1 HALOE CH ₄ and O ₃	14
2.1.2 CLAES N ₂ O	16
2.2 Aircraft Data	16
2.2.1 ALIAS CH ₄	17
2.2.2 Dual-Beam UV-Absorption Photometer O ₃	18
2.3 UKMO PV Data	18
CHAPTER III. MODIFIED LAGRANGIAN-MEAN DIAGNOSTIC FORMALISM	21
3.1 Formulation	22
3.2 Application to Data	28
3.3 Algorithm Testing Using CLAES N ₂ O Data	32

CHAPTER IV. MODIFIED LAGRANGIAN-MEAN DIAGNOSTIC	
APPLIED TO HALOE DATA	36
4.1 Reconstruction of Tracer Distributions	36
4.2 Reconstruction of Daily CH ₄ Distributions and NMLM Results	40
4.3 Validity of the Approach	42
CHAPTER V. TRACER CORRELATIONS	51
5.1 Comparison of Aircraft and Satellite Tracer Correlations	52
5.2 Analysis Using ER-2 Tracer Correlations and HALOE NMLM	
Results	54
CHAPTER VI. SUMMARY AND CONCLUSIONS	66
LIST OF REFERENCES	73

ACKNOWLEDGEMENTS

I wish to express my sincere appreciation to my thesis committee members Drs. William Grose, Mark Hinders, Joel Levine, and Gerald Johnson for their conscientious reading and review of the manuscript. Special thanks are due to Dr. William Grose, my advisor, for his encouragement throughout the pursuit of this degree. I am indebted to him for allowing me to include my thesis research in my job responsibilities. Without his support, guidance, and patience this research would not have been possible.

I would like to thank my co-workers Drs. Jassim Al-Saadi, Richard Eckman, R. Bradley Pierce, Ellis Remsberg, and Mr. T. Duncan Fairlie for their invaluable assistance and suggestions during this endeavor. I also gratefully acknowledge the HALOE and CLAES science team members and the ER-2 instrument team members for providing the satellite and in situ measurements used in this research.

Mr. W. Thomas Blackshear, a retired colleague and personal friend, has my gratitude for our many insightful discussions. He has been an inspiration and huge support for me throughout my career.

Finally, I thank my parents, Edward and Carolyn Lingenfelser for their loving encouragement in all that I pursue. And to my husband, Mr. Uriel "Woody" Lovelace, I owe the greatest thanks for sharing his knowledge with me, for providing his endless support to me, and especially for his patience and understanding as I worked toward this degree.

LIST OF FIGURES

Figure		Page
1.1	Schematic cross section illustrating transport in the lower stratosphere. Heavy solid lines show the mean meridional circulation (Brewer-Dobson cell). Dotted lines indicate quasi-horizontal transport. Crosses show the mean tropopause. EQ, equator; S, summer pole; W, winter pole. (After Holton, 1986.)	4
1.2	Schematic of transport and mixing in the winter hemisphere of the lower stratosphere. Thin lines are isentropic or constant potential temperature surfaces labeled in kelvins. The tropopause is shown by the thick line and where this line is discontinuous denotes the tropopause break region. Stratosphere-troposphere exchange can occur quasi-horizontally in this region. The wiggly double-headed arrows denote quasi-horizontal mixing. The broad arrows show transport by the global-scale circulation. (After Holton <i>et al.</i> , 1995.)	7
3.1	Schematic illustrating the concept of area equivalent latitude. In (a) blue represents the area (A) enclosed by a contour of constant mixing ratio (q), and in (b) red represents the same area (A) centered at the pole and the bounding latitude is the equivalent latitude (ϕ_e).	23
3.2	Schematic of the area (shaded region) enclosed by a tracer contour of mixing ratio q and related parameters. (After Nakamura, 1998.)	26
3.3	NMLM cross section of the CLAES northern hemisphere N ₂ O mixing ratio (ppmv, solid contours) and the natural log normalized equivalent length (color contours) for February 13-19, 1993.	34
3.4	Modified Lagrangian-mean cross section of the CLAES northern hemisphere N ₂ O mixing ratio (vmr, solid contours) and the natural log normalized equivalent length (ξ , color contours) for February 13-19, 1993 generated by Nakamura. (After Nakamura and Ma, 1997.)	35

4.1	NMLM cross section of the CLAES northern hemisphere N ₂ O mixing ratio (ppmv, solid contours) and the natural log normalized equivalent length (color contours) sampled consistent with HALOE observations and then reconstructed using UKMO PV data for February 13-19, 1993.	39
4.2	NMLM cross section of the northern hemisphere HALOE sunset CH ₄ mixing ratio (ppmv, solid contours) and the natural log normalized equivalent length (color contours) reconstructed using UKMO PV for May 5-11, 1992.	41
4.3	NMLM cross section of the CLAES northern hemisphere N ₂ O mixing ratio (ppmv, solid contours) and the natural log normalized equivalent length (color contours) for May 5-11, 1992.	43
4.4	UKMO PV versus HALOE CH ₄ correlation on the 801 K isentropic surface based on data from April 15 through May 19, 1992. Solid line is the average of the CH ₄ data in PV bins. Negative PV values indicate southern hemisphere data.	45
4.5	Polar stereographic map on the 801 K isentropic surface for May 5, 1992 of northern hemisphere (a) PV linearly interpolated to a 4°x4° latitude-longitude grid and to an evenly spaced ln(θ) grid, and (b) HALOE CH ₄ reconstructed using UKMO PV. PV and CH ₄ values are normalized by their corresponding maximum values.	46
4.6	NMLM cross section of northern hemisphere PV ($\times 10^{-2}$ K m ² kg ⁻¹ s ⁻¹ , solid contours) and the natural log normalized equivalent length (color contours) linearly interpolated to a 4°x4° latitude-longitude grid and to an evenly spaced ln(θ) grid for May 5-11, 1992.	48
4.7	NMLM cross section of the northern hemisphere HALOE sunset CH ₄ mixing ratio (ppmv, solid contours) and the natural log normalized equivalent length (color contours) for April 15 through May 19, 1992.	49
5.1	CH ₄ versus O ₃ correlations for October 3-20, 1994 ranging in latitude between 43° and 70° south, ranging in longitude between 147° and 195° east, and covering four potential temperature ranges. Black triangles identify ER-2 data for six flights and red stars identify HALOE sunset data.	53

- 5.2 CH₄ versus O₃ correlation for May 6-20, 1997 ranging in latitude between 61° and 85° north, ranging in longitude between 203° and 258° east, and covering a potential temperature range from 350 to 550 K. Black triangles identify ER-2 data for four flights and red stars identify HALOE sunrise data. 55
- 5.3 ER-2 CH₄ versus O₃ correlation for October 10,13,16, 1994 ranging in latitude between 43° and 70° south, ranging in longitude between 171° and 182° east, and covering a potential temperature range from 350 to 530 K. 57
- 5.4 NMLM cross section of the southern hemisphere HALOE sunset CH₄ mixing ratio (ppmv, solid contours) and the natural log normalized equivalent length (color contours) reconstructed using UKMO PV for October 9-15, 1994. 59
- 5.5 ER-2 CH₄ versus O₃ correlation for May 3, 1993 ranging in latitude between 14° and 38° north, ranging in longitude between 237° and 243° east, and covering a potential temperature range from 410 to 530 K. 62
- 5.6 NMLM cross section of the northern hemisphere HALOE sunset CH₄ mixing ratio (ppmv, solid contours) and the natural log normalized equivalent length (color contours) reconstructed using UKMO PV for April 27-May 3, 1993. 64

ABSTRACT

Observations of methane (CH_4) and ozone (O_3) from both the Halogen Occultation Experiment (HALOE) and the ER-2 aircraft have been used to examine transport characteristics in the lower stratosphere. A modified Lagrangian-mean (NMLM) analysis of the HALOE CH_4 data provided a unique method for identifying so-called transport barriers (i.e., regions where quasi-horizontal transport is inhibited). The NMLM technique can be used with any long-lived tracer provided adequate spatial coverage can be achieved over a reasonably short period. We show how the NMLM technique can be implemented with HALOE occultation data. The HALOE data set is unique in providing an extended record (8 years) of long-lived tracer data. Because the solar occultation sampling pattern of HALOE requires approximately one month to achieve near-hemispheric coverage, synoptic hemispheric distributions of CH_4 are reconstructed through correlations with the United Kingdom Meteorological Office (UKMO) potential vorticity (PV) distributions for 7-day periods which are then analyzed for the presence of transport barriers. The NMLM technique was used to construct area equivalent latitude versus potential temperature cross sections of CH_4 mixing ratio and “equivalent lengths” for these periods. Regions of minimum equivalent length are identified as barrier regions where meridional transport is restricted. Application of this technique to solar occultation data was validated, and it is concluded that the NMLM formalism can be applied to occultation data provided a suitable synoptic distribution of PV can be obtained for the desired period.

Unlike the satellite data, the localized in situ data obtained by instruments aboard aircraft can not be used in the NMLM technique. Instead, correlations between the mixing ratios of various tracer constituents have been used extensively to provide insight into the relative roles of chemistry and transport in the lower stratosphere. However, tracer correlations include the effects of both chemistry and transport and are spatially restricted. Separating the effects of chemistry and transport and accurately interpreting tracer correlations is often difficult. We show that associating an aircraft tracer correlation with a coincident HALOE NMLM analysis provides for a less ambiguous evaluation of the correlations and a more comprehensive approach in studying transport in the lower stratosphere. However, if only one analysis is employed to deduce information about transport, the NMLM technique is preferred to tracer correlations. This analysis not only captures the tracer distribution but also identifies the location, shape and strength of transport barriers and mixing regions. A disadvantage of the method is that it is implemented using global satellite data of lower resolution than the aircraft data. Fortunately, the very good agreement achieved between the aircraft and HALOE CH_4 and O_3 correlations in the lower stratosphere demonstrate that the satellite data can be used confidently in global analyses.

THE USE OF LONG-LIVED TRACER OBSERVATIONS TO EXAMINE
TRANSPORT CHARACTERISTICS IN THE LOWER STRATOSPHERE

CHAPTER I

INTRODUCTION

Studies of the lower stratosphere have taken on new importance since (1) the discovery of the Antarctic ozone (O_3) hole [Farman *et al.*, 1985] and (2) the recognition of midlatitude O_3 trends [WMO, 1999] over the last two decades. These two effects manifest themselves in the lower stratosphere. Here, we use lower stratosphere to denote the region from approximately 22 km down to the tropopause. The need for a better understanding and quantification of O_3 variability has led to a conscious effort to elucidate the relative roles of chemistry and transport. Understanding the role of chemical processes [Salawitch, 1994a,b] is facilitated by direct measurements of chemical species such as those obtained from satellites (see special issue *Journal of the Atmospheric Sciences*, 51, 2781-3108, 1994), airborne platforms (see special sections “SPADE and AASE II,” in *Geophysical Research Letters*, 21, 2535-2610, 1994; “Airborne Southern Hemisphere Ozone Experiment/Measurements for Assessing the Effects of Stratospheric Aircraft,” in *Journal of Geophysical Research*, 102(D3), 3899-3949, 1997), and balloons (see special issue *Journal of Atmospheric Chemistry*, 10, 99-272, 1990). On the other hand, the transport of constituents is more difficult to study in that critical parameters such as global wind distributions are not directly measured. However, the distribution of

chemical species with sufficiently long chemical lifetimes, for example methane (CH_4) and nitrous oxide (N_2O), is determined largely by transport. Therefore, direct observation of these species provides much useful information on transport [*Jones and Pyle, 1984; Roche et al., 1996; Ruth et al., 1994; Ruth et al., 1997*].

Transport in the lower stratosphere is especially intriguing since it is a region of exchange with the troposphere [e.g., *Holton et al., 1995*]. Much of the exchange between the troposphere and stratosphere occurs through the Brewer-Dobson circulation [*Brewer, 1949; Dobson, 1956*]. This circulation is a mean meridional (zonally averaged) circulation which is characterized by tropospheric air ascending across the tropopause in the tropics, drifting poleward in the stratosphere, and ultimately returning to the troposphere in the extratropics [*Andrews et al., 1987*]. The transport of trace chemical species by the mean meridional circulation operates on a time scale of months [*Salby and Garcia, 1990*]. In addition to the slow meridional drift by the Brewer-Dobson circulation in the lower stratosphere, tracers are also subject to large-scale quasi-horizontal motions (planetary-scale disturbances) that operate on much shorter time scales [*Holton, 1992*]. Meridional tracer transport can be affected by these motions depending on their strength and frequency. A schematic illustrating transport in the lower stratosphere is shown in Figure 1.1. This picture has been supported by global satellite measurements of long-lived vertically stratified tracers, where the zonal mean mixing ratio isopleths (i.e., surfaces of constant mixing ratio) in the meridional plane (latitude-height plane) are displaced upward in the tropics and downward in the extratropics [*Jones and Pyle, 1984* see Figures 3 and 4].

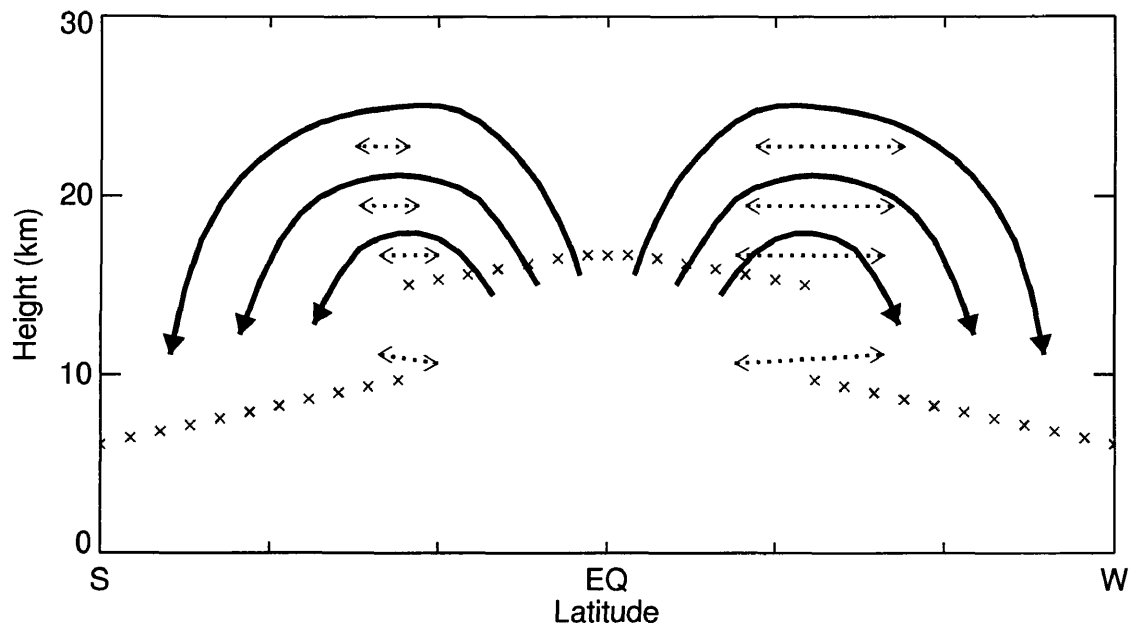


Figure 1.1. Schematic cross section illustrating transport in the lower stratosphere. Heavy solid lines show the mean meridional circulation (Brewer-Dobson cell). Dotted lines indicate quasi-horizontal transport. Crosses show the mean tropopause. EQ, equator; S, summer pole; W, winter pole. (After Holton, 1986.)

In the summer stratosphere when the zonal circulation is easterly, the flow is generally zonally symmetric (i.e., moving parallel to latitude circles about the pole). In contrast, the winter stratosphere is dominated by westerly winds and is dynamically more active with the flow making large meridional excursions. Whenever there are prevailing westerlies during the fall to spring periods, tracers are subject to rapid quasi-horizontal transport and mixing by propagating and eventually breaking planetary-scale Rossby waves. This phenomenon makes studying transport in the winter stratosphere more interesting. The winter hemisphere of the lower stratosphere

can be divided into at least three regions: (1) the low-latitude tropical region, (2) the midlatitude “surf zone” as described by *McIntyre and Palmer* [1983], and (3) the high-latitude polar region. In the tropical region, vertical upwelling from the troposphere is the main mechanism for transport of trace constituents into the stratosphere. Observed tracer distributions show that this region is somewhat isolated from the midlatitude region and that transport out of or into the tropical stratosphere varies with season, altitude, and phase of the quasi-biennial oscillation (QBO) [e.g., *Trepte and Hitchman*, 1992; *Murphy et al.*, 1993; *Volk et al.*, 1996; *O’Sullivan and Dunkerton*, 1997]. *Chen et al.* [1994] and *Waugh* [1996] also show that there are northern and southern hemisphere asymmetries in the lateral transport out of the tropical region. Similar to the tropical region, the polar region is somewhat sequestered from the midlatitude region but only when a polar vortex exists in the winter hemisphere. Vertical downwelling from aloft is the primary transport in this region accompanied by varying degrees of lateral inmixing from and outmixing to lower latitudes [e.g., *Murphy et al.*, 1989; *Pierce and Fairlie*, 1993; *Dahlberg and Bowman*, 1994; *Plumb et al.*, 1994]. There are seasonal, altitude, and hemispheric differences in transport, most notably associated with the extent of the polar vortex [e.g., *Schoeberl et al.*, 1992; *Lahoz et al.*, 1995]. The so-called surf zone is a region affected primarily by the propagation and breaking of planetary-scale Rossby waves. From late fall to early spring when the zonal circulation in the extratropics is westerly, Rossby waves will propagate causing a flow which transports constituents quasi-horizontally, meridionally across latitude circles. If the amplitude of the waves (or disturbances) becomes sufficiently large, the waves “break” [*McIntyre and Palmer*, 1983] and irreversibly deform the tracer

isopleths with resultant quasi-horizontal mixing and a net redistribution of long-lived tracers. Generally, the surf zone is confined to middle latitudes, bounded by the edge of the polar region (the polar vortex edge) and the edge of the tropical region. However, the latitudinal extent this region occupies varies seasonally according to the degree of mixing [*McIntyre and Palmer, 1983; Remsberg and Bhatt, 1996*]. Mixing in the northern hemisphere winter is much more intense than in the southern hemisphere winter due to the hemispheric differences in the surface topography which forces the planetary waves. A schematic of transport and mixing in the winter hemisphere of the lower stratosphere is shown in Figure 1.2.

As mentioned before, the distributions of long-lived tracers reflect large-scale transport. The relatively recent abundance of satellite data such as constituent observations obtained by the National Aeronautics and Space Administration (NASA) Upper Atmosphere Research Satellite (UARS) provides an excellent opportunity to study changes in tracer distributions and identify a variety of transport regimes. Unfortunately, the lower stratosphere is somewhat difficult to study using satellite observations. These measurements tend to have large uncertainties and often have retrieval difficulties because of cloud interference, particularly in the tropics. Airborne observations such as those obtained by the NASA high-altitude ER-2 aircraft also provide extremely useful high-resolution constituent measurements for studying transport in the lower stratosphere. In situ observations are more precise and accurate than the satellite observations, but these data are not global and span short time periods.

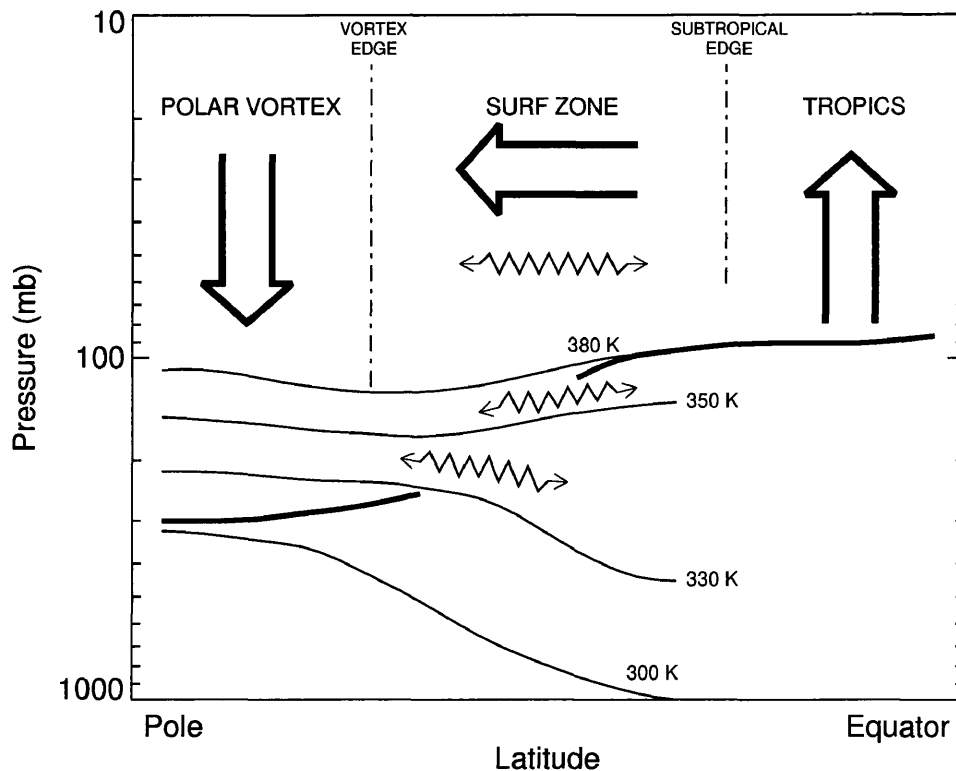


Figure 1.2. Schematic of transport and mixing in the winter hemisphere of the lower stratosphere. Thin lines are isentropic or constant potential temperature surfaces labeled in kelvins. The tropopause is shown by the thick line and where this line is discontinuous denotes the tropopause break region. Stratosphere-troposphere exchange can occur quasi-horizontally in this region. The wiggly double-headed arrows denote quasi-horizontal mixing. The broad arrows show transport by the global-scale circulation. (After Holton *et al.*, 1995.)

Aircraft data have been used extensively to construct correlations between various tracer constituents. Such studies have provided much useful insight into the relative roles of chemistry and transport in the lower stratosphere. For example, tracer

interrelationships have been used to identify O₃ loss and the degree of polar vortex isolation [Proffitt *et al.*, 1989a, 1990], to identify denitrification and dehydration [Fahey *et al.*, 1990a,b], to quantify transport between tropical and middle latitudes [Volk *et al.*, 1996], to examine mixing of polar vortex air into middle latitudes [Vaughan *et al.*, 1997], and to infer transport rates [Boering *et al.*, 1994], generally by interpreting the structure and slope of correlation diagrams (i.e., scatterplots of one tracer versus another). Plumb and Ko [1992] argued that a scatterplot of the mixing ratio of one tracer versus another will collapse to a compact curve provided that the species chemical lifetimes and vertical transport time scales are much longer than quasi-horizontal transport time scales (i.e., species in climatological slope equilibrium). The mixing ratio isopleths of two such tracers are parallel and share a common shape in the meridional plane, with a characteristic poleward-downward slope resulting from a balance between the slope steepening effects at low latitudes of vertical advection by the mean meridional circulation and the slope flattening effects in the extratropical region of quasi-horizontal mixing by large-scale waves [Holton, 1986a,b; Mahlman *et al.*, 1986]. If the tracer correlation is linear, as well as compact, then the species are in gradient equilibrium. In order for this regime to occur the species chemical lifetimes must be very long relative to the vertical transport time scales. Transport processes being much faster than chemical processes assures that the spatial separation of the isopleths of the two tracers, as well as their shape, share a common form [Plumb and Ko, 1992]. Correlations between mixing ratios of any two tracers that are long lived are expected to exhibit compact and linear relationships without regard to latitude or altitude. However, Murphy *et al.* [1993] showed that

tracer interrelationships are not globally uniform and can be substantially different in distinct regions, and in fact, tracer correlations differ in the tropics from those of middle latitudes. Consequently, *Plumb* [1996] states that because mixing is not uniform globally, slope equilibrium does not exist globally even for long-lived tracers, and tracer correlations are compact separately in the isolated tropical region and in the midlatitude surf zone. Therefore, using correlation diagrams for diagnostic purposes is somewhat limited due to complicated interpretation (and sometimes speculation) of what influences the changes in tracer distributions.

The modified Lagrangian-mean formalism developed by Nakamura [*Nakamura*, 1995, 1996, 1998; *Nakamura and Ma*, 1997; *Nakamura et al.*, 1999], hereafter NMLM, is another technique used to examine stratospheric tracer morphology, but can utilize global satellite or model data. The NMLM model is a direct descendant of the *Butchart and Remsberg* [1986] model which uses areas enclosed by tracer isopleths on a given isentropic (constant potential temperature) surface as a coordinate. In essence, quasi-conservative tracers are used as Lagrangian coordinates. Potential temperature acts as the vertical coordinate and the mixing ratio of any stratospheric tracer that has a long chemical lifetime and has coherent meridional gradients on isentropic surfaces acts as the meridional coordinate [*Nakamura*, 1995]. Since such tracers on isentropic surfaces typically have contours that form quasi-concentric loops of monotonically increasing or decreasing mixing ratio around the polar region, the tracer mixing ratio is mapped as a function of the area that its contour encloses at any given time, creating a one-to-one tracer-area relationship [*Nakamura*, 1998]. Consequently, the NMLM diagnostics are viewed in

area-potential temperature coordinates and primarily reflect tracer gradients resulting from differential isentropic mixing and the mixing efficiency [Nakamura and Ma, 1997]. Previously, the NMLM method has been applied using synoptically mapped N_2O data observed by the Cryogenic Limb Array Etalon Spectrometer (CLAES) instrument aboard the UARS and N_2O data simulated by the Geophysical Fluid Dynamics Laboratory's SKYHI general circulation model [see Nakamura and Ma, 1997; Nakamura, 1998; Nakamura *et al.*, 1999]. Here, synoptic is used to denote a set of data that is defined at all spatial positions for discrete times (once daily in this case). These analyses show that the NMLM technique provides a unique method for identifying so-called transport barriers (i.e., regions where quasi-horizontal transport is restricted) and distinguishing the surf zone from the polar and tropical regions.

The goal of this research is to study transport in the lower stratosphere using: (1) aircraft data in tracer correlations; (2) satellite data with the NMLM technique. Long-lived tracers such as CH_4 and N_2O are essential to this research since their distributions are governed primarily by transport. Unfortunately, not a lot of global data for these species are available. The CLAES N_2O data are limited to a time period from October 1991 to May 1993. However solar occultation remote sensing measurements of CH_4 have been obtained since October 1991 by the Halogen Occultation Experiment (HALOE), also aboard UARS. Because of the sparseness and asynchronous character of solar occultation sampling, these data were deemed unsuitable for the NMLM method [Nakamura *et al.*, 1999]. However, global tracer distributions of the HALOE CH_4 can be reconstructed using the synoptic United Kingdom Meteorological Office (UKMO) global potential vorticity (PV) distributions. Here,

the idea is to exploit the correlation between PV (a long-lived dynamical tracer whose global distribution is known) and CH₄ to produce a synoptic distribution of CH₄. It is shown that the reconstruction technique developed can be applied legitimately to any asynoptic data set for a long-lived tracer, provided that near-hemispheric data coverage is obtained within approximately 30 days. The NMLM formalism is then applied to the HALOE reconstructed CH₄ field to facilitate interpretation of tracer transport and mixing in the lower stratosphere. The NMLM results are then compared to aircraft tracer correlations for consistency in interpretation and conclusions.

Organization of this thesis is as follows. A general description of the data used in the analyses is given in Chapter II. Chapter III describes the NMLM diagnostic formalism including the formulation of the transport equation in the area coordinate, application to data, and algorithm testing. Chapter IV focuses on applying the NMLM formalism to very sparse, asynoptic tracer data. The procedure to reconstruct tracer distributions using synoptic PV data is formulated and the validity of the approach is demonstrated. Results from the NMLM analysis of HALOE reconstructed CH₄ distributions are discussed. In Chapter V, two different aspects of tracer correlations (CH₄ and O₃) obtained independently from in situ instruments aboard the ER-2 aircraft and from the HALOE instrument aboard the UARS are discussed. First, the validity of using HALOE data in global transport analyses is assessed using intercomparisons of the aircraft and HALOE tracer correlations. Then, interpretation of aircraft tracer correlations is shown to be less ambiguous when complemented with a HALOE NMLM analysis. Finally, in Chapter VI, a summary of the research is presented, including an assessment of the transport analyses.

CHAPTER II

DATA DESCRIPTION

Long-lived constituents are useful in studying transport. *Collins et al.* [1993] demonstrated that CH_4 and N_2O are equally effective tracers of lower stratospheric motion. Because they are chemically inert in the lower stratosphere, their distributions are primarily determined by transport. Chemical lifetimes in the lower stratosphere of about 30 years for CH_4 and about 100 years for N_2O are long with respect to their transport lifetimes [*Brasseur and Solomon*, 1986]. Both CH_4 and N_2O have sources at the Earth's surface and are well mixed in the troposphere. In the stratosphere, their mixing ratios decrease with height and generally decrease from the equator to the poles. Also, O_3 has a long enough chemical lifetime (~ 1 year) in the lower stratosphere to be an effective dynamical tracer. An exception to this occurs in the chemically perturbed polar vortex, especially the southern hemisphere winter polar vortex. Ozone's primary source is in the equatorial region of the middle stratosphere. In the stratosphere, ozone increases with altitude up to a maximum mixing ratio occurring approximately at 30-38 km depending on latitude and then gradually decreases with altitude.

In this study, we use both aircraft and satellite observations of long-lived constituents to examine transport in the lower stratosphere. Specifically, satellite CH_4

data are used in the NMLM technique and satellite and aircraft CH_4 and O_3 are used in correlations. It is essential that the aircraft and satellite data overlap in time and space in order to check the consistency of what the tracer correlations and NMLM analyses reveal about transport. The aircraft data are available for a number of years and locations, however not a lot of overlapping satellite data are available for these time periods. Nakamura implemented his modified Lagrangian-mean technique with CLAES N_2O data, but these data are limited in time from October 1991 to May 1993. On the other hand, HALOE CH_4 data have been obtained from October 1991 to the present. Unfortunately, the solar occultation sampling pattern of HALOE requires several weeks to obtain near-hemispheric coverage, and the NMLM assumptions make these data unsuitable for use in this technique. Consequently, we exploit the close relationship between potential vorticity and long-lived tracers and use a potential temperature-potential vorticity (PT,PV) coordinate transformation and reconstruction to obtain synoptic hemispheric distributions of HALOE CH_4 . The NMLM technique is then implemented using the HALOE reconstructed CH_4 distributions. These NMLM results are then compared to the aircraft tracer correlations for consistency in interpretation and conclusions.

2.1 Satellite Data

The wealth of data provided by NASA's UARS has substantially advanced stratospheric research in recent years. The UARS was launched by the Space Shuttle on September 12, 1991 and two of its four instruments which measure chemical species, specifically the HALOE and the Microwave Limb Sounder (MLS)

instruments, continue to obtain measurements. The near-circular orbit of UARS at 585 km altitude inclined 57° to the equator combined with the instrument measurement characteristics produces nearly global coverage (that periodically favors the northern and southern hemispheres) throughout the stratosphere and mesosphere [Reber, 1993]. For this research, the extensive spatial and temporal coverage far outweigh the disadvantages associated with satellite measurements such as low horizontal and vertical resolution, and large uncertainties and retrieval difficulties due to clouds in the lower stratosphere.

2.1.1 HALOE CH₄ and O₃

The HALOE instrument [Russell *et al.*, 1993] aboard the UARS conducts remote sensing measurements to obtain vertical profiles of CH₄, O₃, and other trace constituents. The instrument employs the solar occultation technique to obtain sunrise and sunset measurements of constituents, aerosol extinction, and temperature, all as a function of pressure. Species concentrations are inferred by measuring solar attenuation by the limb of the atmosphere as the Sun rises and sets relative to the satellite. Mixing ratios of CH₄ and O₃ are obtained using a gas correlation channel operating in the 3.4 μm region and a broadband radiometer channel centered near 9.8 μm of the ν_3 band, respectively.

HALOE has made observations since October 1991 and continues to operate flawlessly, but in recent years it alternates on/off times with the MLS instrument because of the power constraints that occurred as a result of the loss of one battery and problems with the solar panels on the spacecraft. The occultation technique and the

spacecraft orbital parameters result in approximately 15 sunrise and 15 sunset events each day. On a given day these events occur at approximately constant latitude spaced about 25° apart in longitude. The sunrise and sunset events typically occur in opposite hemispheres [Russell *et al.*, 1993 see Figure 10]. The precessing orbit allows HALOE to sample its full latitude coverage in approximately 36 days and from about 80° south to 80° north over the year [Russell *et al.*, 1993 see Figure 8].

On a clear day, the altitude range extends down from 75 km to about 10 km for CH_4 and from 90 km to about 5 km for O_3 . The vertical resolution is estimated to be 3.5 km for CH_4 and 2.3-2.5 km for O_3 , based upon retrieval simulations conducted by members of the HALOE science team. At altitudes between 15-50 km the horizontal resolution is approximately 6 km x 300 km; that is, the horizontal field of view perpendicular to the line of sight is about 6 km and averages along a limb path of approximately 300 km (L.L. Gordley, HALOE coinvestigator, personal communication, 1999). The version 18 HALOE data are used in this research. The estimated total error (accuracy) is obtained by calculating the root-sum-square of all the random and systematic error mechanisms. Accuracy estimates (L.E. Deaver, HALOE science team, personal communication, 1999) for CH_4 measurements are somewhat smaller than those published in Park *et al.* [1996, see Table 1] for version 17, which vary from 15% at 40 mbar (~ 22 km) to 19% at 100 mbar (~ 16 km). However, accuracy estimates for O_3 measurements should be very nearly the same as those for version 17 which vary from 18% at 40 mbar to 30% at 100 mbar [Bruhl *et al.*, 1996 see Table 1]. In the 40-100 mbar region, the precision is better than 11% for both CH_4 and O_3 measurements. At altitudes below the 100 mbar level, the estimated

errors in CH₄ and O₃ are variable and greater than those at the 100 mbar level.

2.1.2 CLAES N₂O

The CLAES instrument [Roche *et al.*, 1993] aboard the UARS obtained vertical profiles of N₂O for 19 months, from October 1, 1991 to May 5, 1993. The CLAES lifetime was limited by the finite amount of stored cryogen used to cool the instrument. However, CLAES is a limb sounding instrument whose measurements provide near-hemispheric coverage per day. The NMLM formalism in this study is applied to the N₂O data strictly to test the software by duplicating Nakamura's results [Nakamura and Ma, 1997]. Also, these data were very useful in testing the logic and feasibility of reconstructing constituent distributions using the UKMO PV distributions. Since the spatial distributions of both CH₄ and N₂O are determined mainly by transport and have very similar morphology, results of the NMLM analyses using these two species are expected to be comparable.

The CLAES N₂O data used are the version 7, level-3AL mapped products (data interpolated to a common UARS grid and latitude referenced). The measurement characteristics of these data are detailed by Roche *et al.* [1996].

2.2 Aircraft Data

In situ measurements obtained by NASA's high-altitude ER-2 aircraft provide high-resolution, and highly precise and accurate constituent distributions along the aircraft flight path. ER-2 sampling during the 1991-1992 Airborne Arctic Stratospheric Expedition II (AASE II), 1992-1993 Stratospheric Photochemistry,

Aerosols and Dynamics Expedition (SPADE), 1994 Airborne Southern Hemisphere Ozone Experiment/Measurements for Assessing the Effects of Stratospheric Aircraft (ASHOE/MAESA), 1995-1996 Stratospheric Tracers of Atmospheric Transport (STRAT), and 1997 Photochemistry of Ozone Loss in the Arctic Region in Summer (POLARIS) campaigns renders an extensive set of in situ CH₄ and O₃ measurements. These data range in altitude from the ground to approximately 21 km and cover a wide range of latitude and season. In the time period from August 1991 through September 1997, the ER-2 aircraft accomplished a total of 191 flights, of which 95 flights successfully obtained CH₄ and O₃ data from the Aircraft Laser Infrared Absorption Spectrometer (ALIAS) and dual-beam UV-absorption photometer instruments, respectively. The flights included test flights from Ames Research Center, California; transit flights to/from the deployment sites; and flights from and returning to the deployment sites.

2.2.1 ALIAS CH₄

The ALIAS instrument is a scanning tunable diode laser spectrometer [*Webster et al.*, 1994] which directly measures CH₄ from the ER-2 aircraft, using high resolution laser absorption at infrared wavelengths in a multipass cell. Basically, this instrument transmits light emitted from lasers operating in the 3.4 to 8 μm wavelength range into a 1 meter long absorption cell containing an atmospheric air sample. After traversing 80 passes (80 meter path length) of the cell, the beams exit to detectors which determine the amount of radiation transmitted through the absorption cell and thus creating an absorption spectrum. The concentration of CH₄ is then determined

using this spectrum and the laboratory deduced CH₄ absorption cross section. For a response time (data rate) of 3 seconds the precision is 1% for the in situ CH₄. The reported accuracy of the measurements is 5%.

2.2.2 Dual-Beam UV-Absorption Photometer O₃

A dual-beam UV-absorption photometer [Proffitt and McLaughlin, 1983; Proffitt *et al.*, 1989b] was used to obtain in situ O₃ measurements from the ER-2 during several aircraft campaigns. This instrument transmits 254 nm radiation to detectors through two identical absorption chambers, one containing a sample of O₃ rich air and the other containing air scrubbed of O₃. Since O₃ strongly absorbs 254 nm radiation and its absorption cross section is well known, O₃ number density is readily calculated after comparing the signals detected in each chamber. Subsequently, the O₃ mixing ratio can be determined using the chamber temperature and pressure measurements. Nearly continuous measurements are made by systematically (once every 10 seconds) interchanging the O₃ rich air sample and the air sample free of O₃ between the two chambers. For a response time of 1 second the precision (minimum detectable concentration) for O₃ is 1.5×10^{10} molecules/cm³, approximately 1% of a typical stratospheric abundance. The reported accuracy of the measurements is 3% plus precision.

2.3 UKMO PV Data

Ertel's potential vorticity [Andrews *et al.*, 1987], is a quasi-conservative tracer in the lower stratosphere. That is, PV remains approximately constant following the

motion of an air parcel in adiabatic frictionless flow and is an excellent tracer for motions on time scales of less than a few weeks. Analytically [Holton, 1992], PV is the absolute vorticity (i.e., component of relative vorticity normal to an isentropic surface plus the Coriolis parameter which is twice the local vertical component of Earth's angular velocity) multiplied by a term which is regarded as a local measure of the depth of the layer between two isentropic surfaces. In a sense, PV is a measure of the ratio of the rotation of a fluid column to the depth of the column and is the compressible fluid-dynamical analogue of conservation of angular momentum for solid body rotation. Since the isentropic distributions of this quasi-conservative tracer are similar to CH₄ distributions, PV is used in this research to construct synoptic hemispheric distributions of HALOE CH₄.

The UKMO PV data used in reconstructing HALOE CH₄ distributions are accessed from a NASA Langley Research Center archive of PV on isentropic surfaces. The PV data are calculated from temperatures and winds obtained from daily assimilated analyses produced by the UKMO for the UARS project. The assimilated temperatures and winds are available on 22 UARS pressure surfaces ranging from 1000 mbar up to 0.3 mbar, on a 2.5° latitude grid ranging from 88.75° south to 88.75° north, and on a 3.75° longitude grid ranging from 1.875° to 358.125° east. These data and details of the UKMO data assimilation system are described by *Swinbank and O'Neill* [1994].

Potential vorticity is calculated at the UARS pressure levels and then linearly interpolated onto 35 isentropic surfaces ranging: 240 to 400 every 10 K, 400 to 550 every 25 K, 600 to 1000 every 100 K, and 1000 to 2400 every 200 K. The PV latitude

and longitude grids are the same as those for the assimilated data. Daily files of synoptic PV are usually archived on a quarterly basis and are available from October 17, 1991 to very nearly the present time (R.B. Pierce and V.L. Harvey, personal communication, 1999).

CHAPTER III

MODIFIED LAGRANGIAN-MEAN DIAGNOSTIC FORMALISM

Nakamura developed a two-dimensional modified Lagrangian-mean technique of tracer transport in the stratosphere using potential temperature and the area enclosed by contours of constant tracer mixing ratio on isentropic surfaces as vertical and meridional coordinates, respectively [Nakamura, 1996]. The NMLM formalism is an extension of the *Butchart and Remsberg* [1986] area diagnostic and casts tracer transport in a Lagrangian vertical cross section revealing regions of varying degrees of quasi-horizontal isentropic transport and mixing.

On isentropic surfaces, the hemispheric distributions of long-lived tracers generally form quasi-concentric contours of monotonically increasing or decreasing mixing ratio around the pole. By associating each tracer contour with the area it encloses at a given time, a one-to-one tracer-area relationship is established [Nakamura, 1998]. In order to give the meridional coordinate the sense of latitude, area equivalent latitude ϕ_e [Butchart and Remsberg, 1986; Nakamura 1995] is defined as the bounding latitude of a circle centered at the pole whose enclosed area represents the area enclosed by a tracer contour of constant mixing ratio, i.e.,

$$\phi_e = \sin^{-1}[(1 - A)/(2\pi r^2)] \quad , \quad (3.1)$$

where A is the area enclosed by a specific tracer contour, and r is the mean radius of

the Earth (see Figure 3.1). Consequently, the NMLM technique is used to construct area equivalent latitude versus potential temperature cross sections of tracer mixing ratio and equivalent length which provides a unique way of identifying regions where quasi-horizontal transport is restricted.

3.1 Formulation

In the lower stratosphere, it is convenient to use potential temperature θ as a vertical coordinate [Andrews *et al.*, 1987] since parcels remain on constant potential temperature surfaces for motions that are isentropic (i.e., adiabatic). Also, when using isentropic coordinates the vertical velocity is equivalent to the diabatic heating term Q , and thus transport across isentropic surfaces is easily separated from transport along isentropic surfaces [Holton *et al.*, 1995]. *Haltiner and Williams* [1980] show that the mass continuity equation in isentropic coordinates is given by

$$\frac{d}{dt} \left(\ln \left(\frac{\partial p}{\partial \theta} \right) \right) + \nabla \cdot \mathbf{V} + \frac{\partial Q}{\partial \theta} = 0 \quad , \quad (3.2)$$

where p is pressure, ∇ is the two-dimensional gradient operator on an isentropic surface, \mathbf{V} is the two-dimensional horizontal velocity vector, and Q is $d\theta/dt$.

Following the formulation of *Fairlie* [1993], the continuity equation for tracer mixing ratio q can be expressed as

$$\frac{dq}{dt} \equiv \frac{\partial q}{\partial t} + \mathbf{U} \cdot \nabla_{3D} q = S + K \quad , \quad (3.3)$$

where \mathbf{U} is the three-dimensional velocity vector, ∇_{3D} is the three-dimensional gradient operator, S represents chemical source/sink terms, and K represents small-

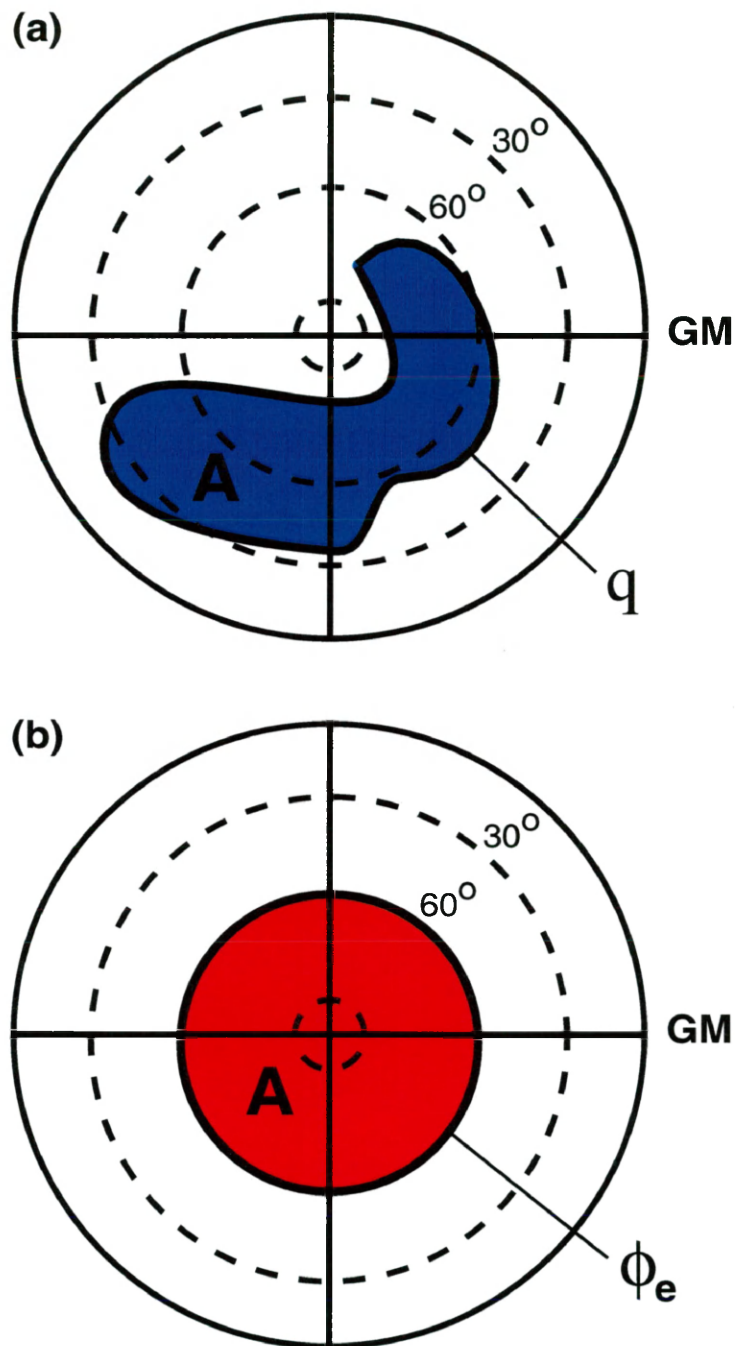


Figure 3.1. Schematic illustrating the concept of area equivalent latitude. In (a) blue represents the area (A) enclosed by a contour of constant mixing ratio (q), and in (b) red represents the same area (A) centered at the pole and the bounding latitude is the equivalent latitude (ϕ_e).

scale processes. The presence of K indicates that mixing ratio even for long-lived tracers is not exactly conserved following parcel motion. Separating the horizontal and vertical components, Equation 3.3 can be rewritten as

$$\frac{dq}{dt} \equiv \frac{\partial q}{\partial t} + \mathbf{V} \cdot \nabla q + Q \frac{\partial q}{\partial \theta} = S + K . \quad (3.4)$$

Multiplying Equation 3.2 by q and adding to Equation 3.4 gives

$$\frac{\partial q}{\partial t} + q \frac{d}{dt} \left(\ln \left(\frac{\partial p}{\partial \theta} \right) \right) + \nabla \cdot (q \mathbf{V}) + \frac{\partial}{\partial \theta} (q Q) = S + K$$

or

$$\frac{\partial q}{\partial t} + \mathbf{V} \cdot \nabla q + Q \frac{\partial q}{\partial \theta} = S + K . \quad (3.5)$$

The characteristics of the lower stratosphere allow assumptions that simplify the tracer continuity equation (Equation 3.5). For relatively short time scales (i.e., characteristic time over which flow can be considered isentropic), the NMLM formalism assumes that (1) the diabatic transport associated with cross-isentropic flow is much slower than the isentropic transport and can be neglected, and (2) the distribution of long-lived tracers is determined mainly by transport and chemical production and loss can be neglected. Also, the stratospheric winds are assumed to be nearly nondivergent on isentropic surfaces. Neglecting the slower process mentioned above, Equation 3.5 reduces to the form

$$\frac{\partial q}{\partial t} + \mathbf{V} \cdot \nabla q = K . \quad (3.6)$$

The expression for K is defined [Nakamura, 1996, 1998] as

$$K = \nabla \cdot (D \nabla q) = D \nabla^2 q , \quad (3.7)$$

where D is a constant coefficient representing microscale diffusion, and $\nabla^2 q$ is the Laplacian of q on an isentropic surface. Here, diffusion is not the “true” diffusion that occurs at the molecular level due to the random motion of atoms and molecules [Brasseur and Solomon, 1986]. This microscale diffusion term is merely used to represent the transport occurring on unresolved scales.

Adopting the Nakamura scheme, a transport equation in the area coordinate is derived using the tracer continuity equation (Equation 3.6). First, tracer mixing ratio q is associated with the area A its contour encloses on an isentropic surface at a given time t . This area includes mixing ratios that are equal to and less than q (i.e., area of the region where $q^* \leq q$) and is determined by evaluating

$$A(q, t) = \mathcal{A}(q), \quad (3.8)$$

where \mathcal{A} is an area integral operator and defined as

$$\mathcal{A}(\dots) \equiv \int \int_{q^* \leq q} (\dots) dA = \int_{q_{\min}}^q dq^* \oint_{q^*} \frac{(\dots)}{|\nabla q|} dl . \quad (3.9)$$

A schematic of the area enclosed by a tracer contour of mixing ratio q and related parameters is shown in Figure 3.2.

The continuity equation in the tracer (q) coordinate is then determined using the identity [Nakamura, 1998 see Appendix]

$$\frac{\partial}{\partial t} \int \int_{q^* \leq q} (\dots) dA = -\frac{\partial}{\partial q} \int \int_{q^* \leq q} (\dots) \frac{\partial q}{\partial t} dA + \int \int_{q^* \leq q} \frac{\partial}{\partial t} (\dots) dA \quad (3.10)$$

and substituting $\partial q / \partial t$ from Equation 3.6 to yield

$$\frac{\partial}{\partial t} A(q, t) = \frac{\partial}{\partial q} \int \int_{q^* \leq q} \mathbf{V} \cdot \nabla q dA - \frac{\partial}{\partial q} \int \int_{q^* \leq q} D \nabla^2 q dA . \quad (3.11)$$

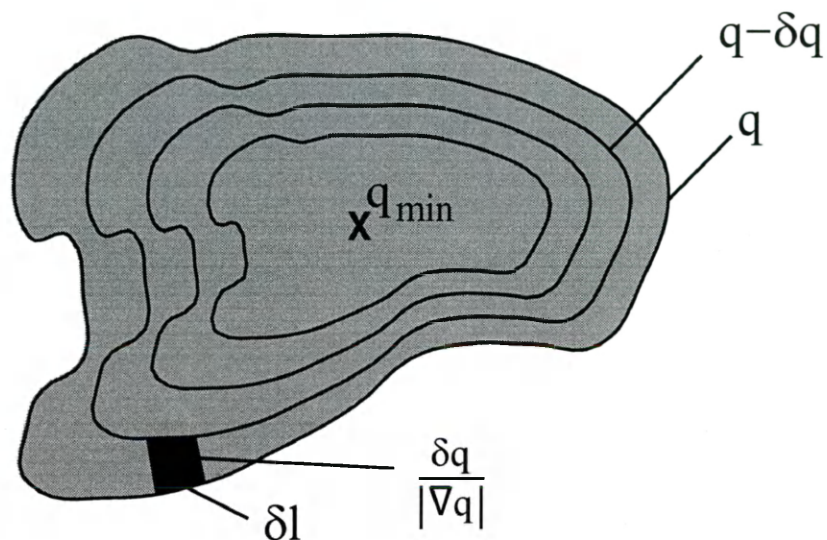


Figure 3.2. Schematic of the area (shaded region) enclosed by a tracer contour of mixing ratio q and related parameters. (After Nakamura, 1998.)

However, horizontal advection by nondivergent winds does not affect the area [Nakamura *et al.*, 1999], and the following logic shows that the first term on the right-hand-side of this equation vanishes. Since

$$\frac{\partial}{\partial q} \int \int_{q^* \leq q} (\dots) dA = \oint_q \frac{(\dots)}{|\nabla q|} dl, \quad (3.12)$$

then

$$\frac{\partial}{\partial q} \int \int_{q^* \leq q} \mathbf{V} \cdot \nabla q dA = \oint_q \frac{\mathbf{V} \cdot \nabla q}{|\nabla q|} dl,$$

and using the divergence theorem, which relates the area integral to the line integral, allows the flux of \mathbf{V} over a q contour to equal the divergence of \mathbf{V} over the area inside q , i.e.,

$$\oint_q \mathbf{V} \cdot \frac{\nabla q}{|\nabla q|} dl = \int \int_{q^* \leq q} \nabla \cdot \mathbf{V} dA .$$

Since winds are assumed to be nondivergent, $\nabla \cdot \mathbf{V} = 0$ and Equation 3.11 reduces to

$$\frac{\partial}{\partial t} A(q, t) = - \frac{\partial}{\partial q} \int \int_{q^* \leq q} D \nabla^2 q dA . \quad (3.13)$$

Finally, considering the one-to-one relationship between the area A and tracer q the continuity equation in the tracer coordinate is inverted to yield the transport equation in the area coordinate:

$$\begin{aligned} \frac{\partial}{\partial t} q(A, t) &= - \frac{\partial}{\partial t} A(q, t) \times \frac{\partial q}{\partial A} \\ &= \frac{\partial}{\partial A} \int \int_{q^* \leq q} D \nabla^2 q dA = D \frac{\partial}{\partial A} \int \int_{q^* \leq q} \nabla \cdot \nabla q dA . \end{aligned} \quad (3.14)$$

Using the divergence theorem and the relation in Equation 3.12, Equation 3.14 can be rewritten as

$$\frac{\partial}{\partial t} q(A, t) = D \frac{\partial}{\partial A} \oint_q \nabla q \cdot \frac{\nabla q}{|\nabla q|} dl$$

and

$$\frac{\partial}{\partial t} q(A, t) = D \frac{\partial}{\partial A} \left[\frac{\partial}{\partial q} \int \int_{q^* \leq q} |\nabla q|^2 dA \right] , \quad (3.15)$$

respectively. Multiplying and dividing Equation 3.15 by $\partial q / \partial A$ gives

$$\frac{\partial}{\partial t} q(A, t) = D \frac{\partial}{\partial A} \left(\left[\frac{\partial}{\partial A} \int \int_{q^* \leq q} |\nabla q|^2 dA \right] \left[\frac{\partial q}{\partial A} \right]^{-1} \right) . \quad (3.16)$$

By defining an equivalent length L_e [Nakamura, 1996], Equation 3.16 can be

expressed as

$$\frac{\partial}{\partial t} q(A, t) = D \frac{\partial}{\partial A} \left[L_e^2 \frac{\partial q}{\partial A} \right], \quad (3.17)$$

where

$$L_e^2 = \left[\frac{\partial}{\partial A} \int \int_{q^* \leq q} |\nabla q|^2 dA \right] \left(\frac{\partial q}{\partial A} \right)^{-2}, \quad (3.18)$$

and Equation 3.17 is the NMLM transformation of Equation 3.6.

The equivalent length [Nakamura, 1996, 1998] is approximately equal to the perimeter length of the q contour that encloses area A and is a useful measure of the efficiency of irreversible transport. Regions of large equivalent length (i.e., substantial stretching of the tracer contours) are associated with rapid quasi-horizontal transport and mixing, whereas, regions of minimum equivalent length are identified as barrier regions where meridional transport is restricted. Thus, equivalent length (and its square) is a key diagnostic in the NMLM model.

3.2 Application to Data

This section describes the procedure used to analyze tracer data according to the NMLM formalism [Nakamura *et al.*, 1999] and provides a detailed outline for implementing the technique. The NMLM technique requires that data coverage be at least hemispheric in order to establish the tracer-area relationship, and ideally the tracer data should be synoptic and global. Unfortunately, this type of coverage is rarely obtained from satellite observations, and often there are no measurements in the polar regions. Assuming daily measurements of temperature and tracer mixing ratio

exist on a latitude-longitude-pressure grid, steps (1) through (6) outlined below are implemented per day to prepare the tracer data for the NMLM calculations.

- (1) Calculate potential temperature, θ , at each grid point.
- (2) Linearly interpolate the tracer data onto specific isentropic surfaces at each horizontal grid point in the hemisphere. The specified isentropic surfaces are chosen such that they span certain regions of the stratosphere evenly in $\ln(\theta)$. Note that the equator should not be viewed as a boundary since closed contours of constant tracer mixing ratio often cross the equator into the opposite hemisphere. Consequently, the hemispheric data should include tracer measurements to approximately 10° latitude in the opposite hemisphere.
- (3) On each isentropic surface, linearly interpolate the tracer data onto equally spaced longitude and/or latitude grids if the data are on irregular grids.
- (4) Fourier transform in longitude if tracer data are missing in the polar region or if the grid spacing in longitude is not equal to the grid spacing in latitude.
- (5) Fill the polar region that lacks data by interpolating the surrounding data [*Nakamura and Ma, 1997* see Appendix]. Specifically, each Fourier coefficient is interpolated into the dataless latitudes from the lower latitudes using a cubic spline method. Constraints at the pole are (1) all Fourier coefficients vanish at the pole for zonal wavenumbers 1 or greater (create asymmetric coefficient arrays as a function of co-latitude to satisfy), and (2) the gradient of the Fourier coefficient vanishes at the pole for the zonal mean (create symmetric coefficient array as a function of co-latitude to satisfy).
- (6) Inverse Fourier transform using the Fourier coefficients to obtain tracer grid

point values in the polar region and/or to obtain tracer grid point values at longitudes whose grid spacing is consistent with the latitude grid spacing. Note that equal grid spacing in latitude and longitude minimizes the directional bias in the horizontal tracer gradient calculation.

The NMLM calculations are performed on the regridded tracer distributions that are functions of latitude, longitude, potential temperature, and day. The tracer-area relationship and the squared equivalent length are calculated on each isentropic surface as follows in steps (7) through (15).

- (7) Calculate the horizontal tracer gradient and its square, $|\nabla q|^2$ at each grid point using centered finite differences (one-sided differences at boundaries).
- (8) Determine the minimum and maximum tracer mixing ratio values (include all days) and define 100 equally spaced tracer contour levels (q contours) between these values. The contour levels must range from minimum to maximum mixing ratio in order to span the entire hemisphere appropriately.
- (9) For each day, determine the area enclosed by each tracer contour level defined above. A surface area is associated with each tracer grid point. This area depends on the latitude and longitude grid spacing and changes only with latitude. The total area enclosed by a specific tracer contour level is obtained by summing the areas associated with tracer mixing ratios that are equal to or less than the q contour. Note that area must be integrated (summed) from pole to equator, and therefore in this case, the data are assumed to have a minimum at the pole and increase toward the equator.
- (10) For each day, integrate the squared horizontal tracer gradient over the area

enclosed by each tracer contour level, i.e., $\int \int_{q^* \leq q} |\nabla q|^2 dA$.

Multiply the squared horizontal tracer gradient and the associated surface area at each grid point, and then sum this product over the grid points where the tracer mixing ratios are equal to or less than the q contour.

- (11) For each tracer contour level, aggregate the area enclosed by the q contour and aggregate the integrated squared horizontal tracer gradient over approximately 6 to 8 consecutive days and calculate the mean area, $A(q)$, and mean gradient, $G(q)$, (i.e., divide by number of days) to remove random errors.
- (12) For each tracer contour level, calculate the area equivalent latitude, $\phi_e(q)$, using the area $A(q)$ and Equation 3.1.
- (13) For each tracer contour level, calculate the squared equivalent length, $L_e^2(q)$, from the area enclosed by the q contour, $A(q)$, and the squared horizontal tracer gradient integrated over this area, $G(q)$, i.e.,

$$L_e^2 = \frac{\partial G}{\partial A} \left(\frac{\partial q}{\partial A} \right)^{-2} . \quad (3.19)$$

Note that Equation 3.19 is equivalent to Equation 3.18. Using centered finite differences to evaluate L_e^2 , Equation 3.19 is approximated by

$$L_e^2 = [A(q + \delta q) - A(q - \delta q)] \times [G(q + \delta q) - G(q - \delta q)] / (2\delta q)^2 , \quad (3.20)$$

where δq is the increment between the equally spaced q contours. One-sided finite differences are taken at the boundaries (i.e., at the minimum and maximum contour levels).

- (14) Linearly interpolate to obtain the tracer mixing ratio and squared equivalent length as a function of area equivalent latitude. Since the measured area

(equivalent latitude) is usually unevenly spaced with respect to the q contours, the mixing ratio as well as the squared equivalent length must be interpolated onto a regularly gridded area equivalent latitude, ϕ_e , coordinate. Note that the interpolations are from the tracer coordinate onto the area (equivalent latitude) coordinate.

- (15) Normalize the squared equivalent length and determine the natural logarithm, i.e.,

$$\xi = \ln (L_e^2 / L_0^2), \quad (3.21)$$

where $L_0^2 = 2\pi r \cos \phi_e$ is the circumference of the zonal circle at equivalent latitude ϕ_e . This step allows the squared equivalent length to be viewed in a nondimensional form. Note that since equivalent length is approximately equal to the perimeter length of a contour of constant mixing ratio, $\xi=0$ if this contour coincides with the zonal circle and ξ will grow as this contour becomes more stretched and deformed [Nakamura and Ma, 1997]. Applying these steps to observed data provides a numerically simple procedure for analyzing the tracer mixing ratio and equivalent length of its contours in the area equivalent latitude versus potential temperature coordinate.

3.3 Algorithm Testing Using CLAES N₂O Data

Nakamura applied his modified Lagrangian-mean technique using the CLAES (version 7, level 3AL) N₂O data averaged over 6 to 8 days to diagnose barrier regions [Nakamura and Ma, 1997; Nakamura et al., 1999]. Both hemispheres were analyzed for several months between February 1992 and February 1993 to observe the summer-

to-winter and the winter-to-summer barrier migration. We simply use these results to validate the software developed to implement the NMLM technique. The procedure outlined in the previous section is applied to the same CLAES N₂O data used by Nakamura, and the results are displayed as area equivalent latitude versus potential temperature cross sections. For all time periods and for both hemispheres, Nakamura's results are very closely duplicated. The comparison of our results, shown in Figure 3.3, to those of Nakamura, shown in Figure 3.4, is typical of how well we duplicate the NMLM algorithm. The small deviations in the results are deemed not significant and are most likely due to using different routines to perform linear and spline interpolations, Fourier transformations, and contour plotting. Therefore, it is concluded that our software successfully implements Nakamura's modified Lagrangian-mean formalism.

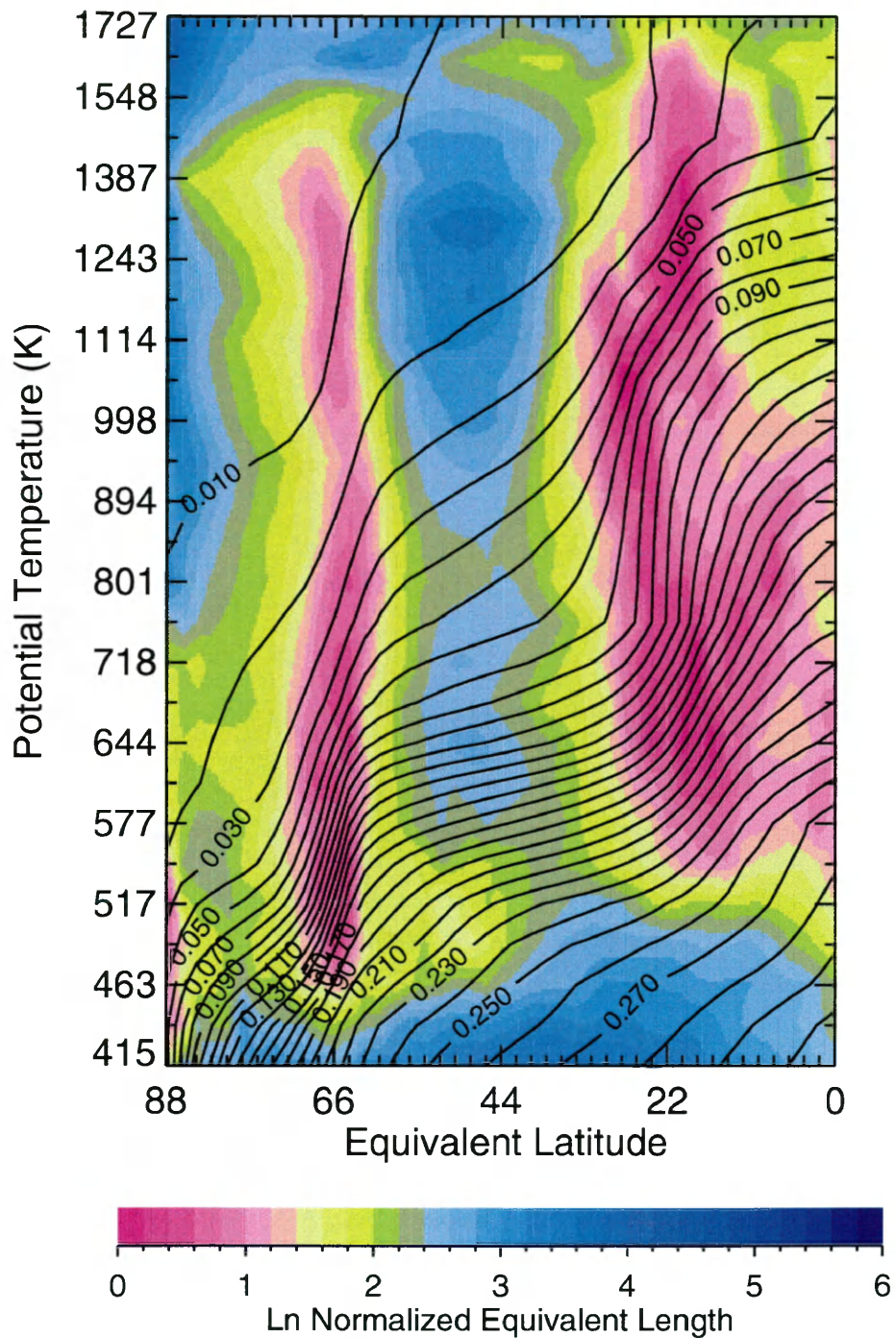


Figure 3.3. NMLM cross section of the CLAES northern hemisphere N_2O mixing ratio (ppmv, solid contours) and the natural log normalized equivalent length (color contours) for February 13-19, 1993.

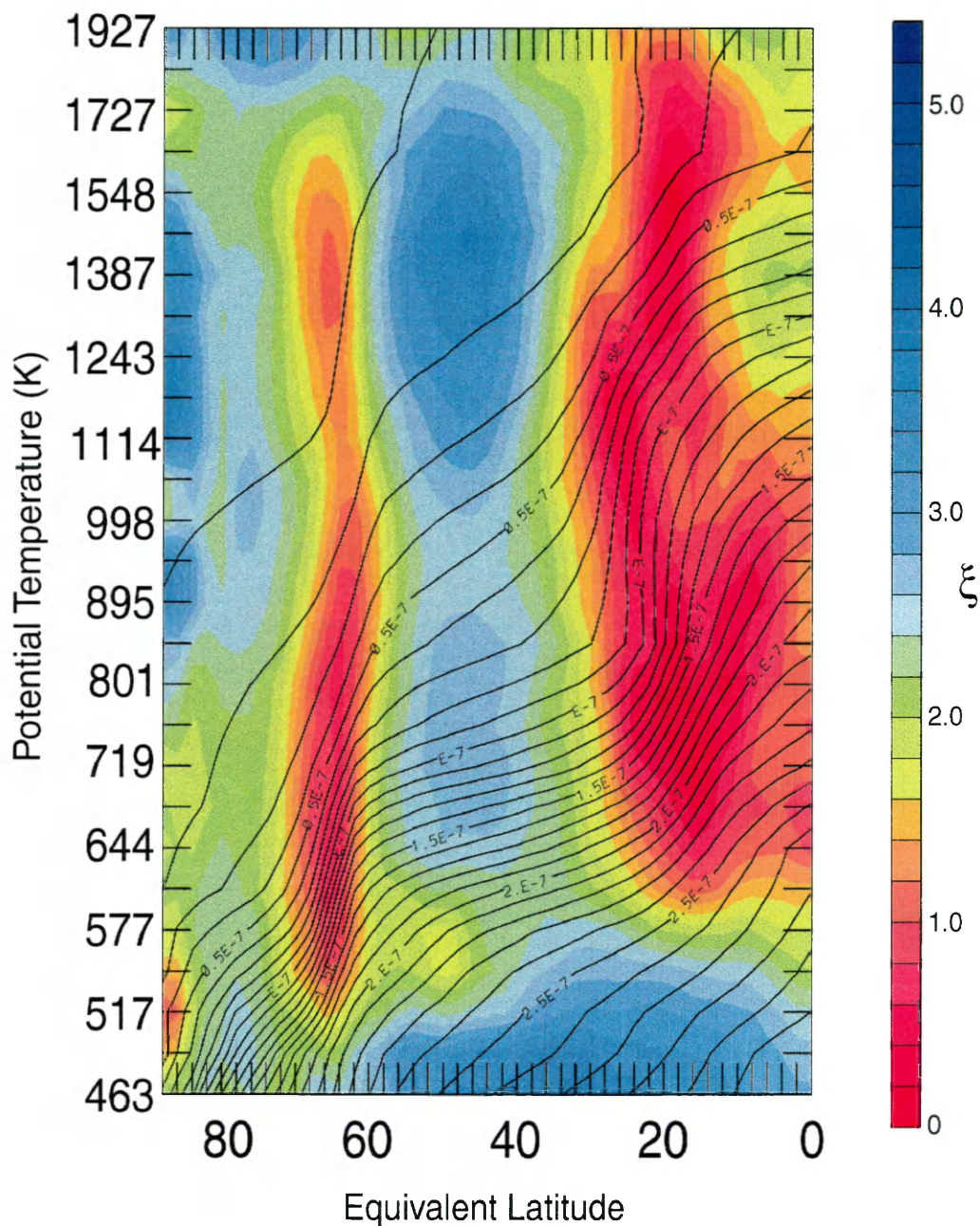


Figure 3.4. Modified Lagrangian-mean cross section of the CLAES northern hemisphere N₂O mixing ratio (vmr, solid contours) and the natural log normalized equivalent length (ξ , color contours) for February 13-19, 1993 generated by Nakamura. (After Nakamura and Ma, 1997.)

CHAPTER IV

MODIFIED LAGRANGIAN-MEAN DIAGNOSTIC APPLIED TO HALOE DATA

The NMLM technique can be used with any long-lived tracer provided adequate spatial coverage can be achieved over a reasonably short period of time (i.e., characteristic time over which flow can be considered isentropic, approximately 7-10 days in the lower stratosphere [see *McIntyre and Palmer, 1983*]). This chapter shows how the NMLM technique can be implemented with occultation data. The HALOE data set is unique in providing an extended record (8 years) of long-lived tracer data. Because the solar occultation sampling pattern of HALOE requires approximately one month to achieve near-hemispheric coverage, synoptic hemispheric distributions of CH₄ are reconstructed through correlations with the UKMO PV distributions for 7-day periods which are then analyzed for the presence of transport barriers.

4.1 Reconstruction of Tracer Distributions

This section describes the potential temperature-potential vorticity coordinate transformation and reconstruction to determine synoptic tracer distributions from a set of HALOE occultation observations using the UKMO analyses for PV. Files of synoptic distributions of PV are archived at NASA Langley Research Center and are available from October 17, 1991 to very nearly the present time (see Chapter 2). The

PV files are accessed on a daily basis corresponding to time periods associated with the tracer time range. The tracer time range is selected to achieve near-hemispheric coverage and is not less than 7 days. Assuming daily measurements of tracer mixing ratio exist on a latitude-longitude-theta grid, the steps outlined below are implemented to reconstruct the tracer distributions.

- (1) For each day, linearly interpolate the tracer data onto isentropic surfaces (corresponding to those defined for the UKMO PV) at each horizontal grid point in the hemisphere. Note that the hemispheric data should include tracer measurements to approximately 10° latitude in the opposite hemisphere.
- (2) For each day in the desired time period, linearly interpolate the PV data onto the same latitude and longitude grids as the tracer data.
- (3) Determine the tracer field in potential temperature-potential vorticity space. For each isentropic surface, use the PV versus tracer correlation to bin the tracer data in PV bins (include all days in the desired period) and determine the average tracer mixing ratio value per bin. Normally, between 10 and 30 equally spaced PV bins are defined between the minimum and maximum PV values on an isentropic surface. For each PV bin, the tracer data that fall within the bin are averaged and associated with the PV value at the midpoint of the bin. Processing all bins and all isentropic surfaces produces a tracer field as a function of potential temperature and PV.
- (4) Transform the tracer field in potential temperature-potential vorticity space back into real (latitude-longitude-theta) space. Using the tracer data determined above and the daily archived UKMO PV data corresponding to 7

consecutive days within the tracer time period, linearly interpolate in PV to get the tracer data at the UKMO PV locations (i.e., tracer mixing ratio as a function of UKMO latitude, longitude, potential temperature, and day).

- (5) For each day, linearly interpolate the tracer data which is on the UKMO grid onto a latitude-longitude-theta grid with consistent grid spacing in latitude and longitude and evenly spaced in $\ln(\theta)$.

The NMLM calculations can then be performed on the reconstructed tracer distributions following steps (7) through (15) in Chapter 3.

The CLAES instrument obtains near-hemispheric measurements on a daily basis. Therefore, the CLAES data does not need to be reconstructed. However, to demonstrate the efficacy of the reconstruction technique, the CLAES N₂O data from February 12 through March 16, 1993 were sampled in a manner consistent with HALOE observations and then reconstructed and used to test the logic outlined in the steps above. The NMLM results using the HALOE-sampled CLAES N₂O data reconstructed from UKMO PV data for February 13-19, 1993 are shown in Figure 4.1. These results are comparable to the NMLM results using the CLAES N₂O data that are not reconstructed (see Figure 3.3) but not without some discrepancies. Both analyses show polar and subtropical barriers of approximately the same size, strength, and equivalent latitude location. However, the vertical extent of these barriers is greater for the reconstructed case. At the lowest altitudes (below ~470 K), a pool of large equivalent lengths crossing most equivalent latitudes seen in the actual CLAES data seems inconsistent with the isentropic tracer gradients (i.e., usually large equivalent lengths are associated with small isentropic gradients) and is not duplicated

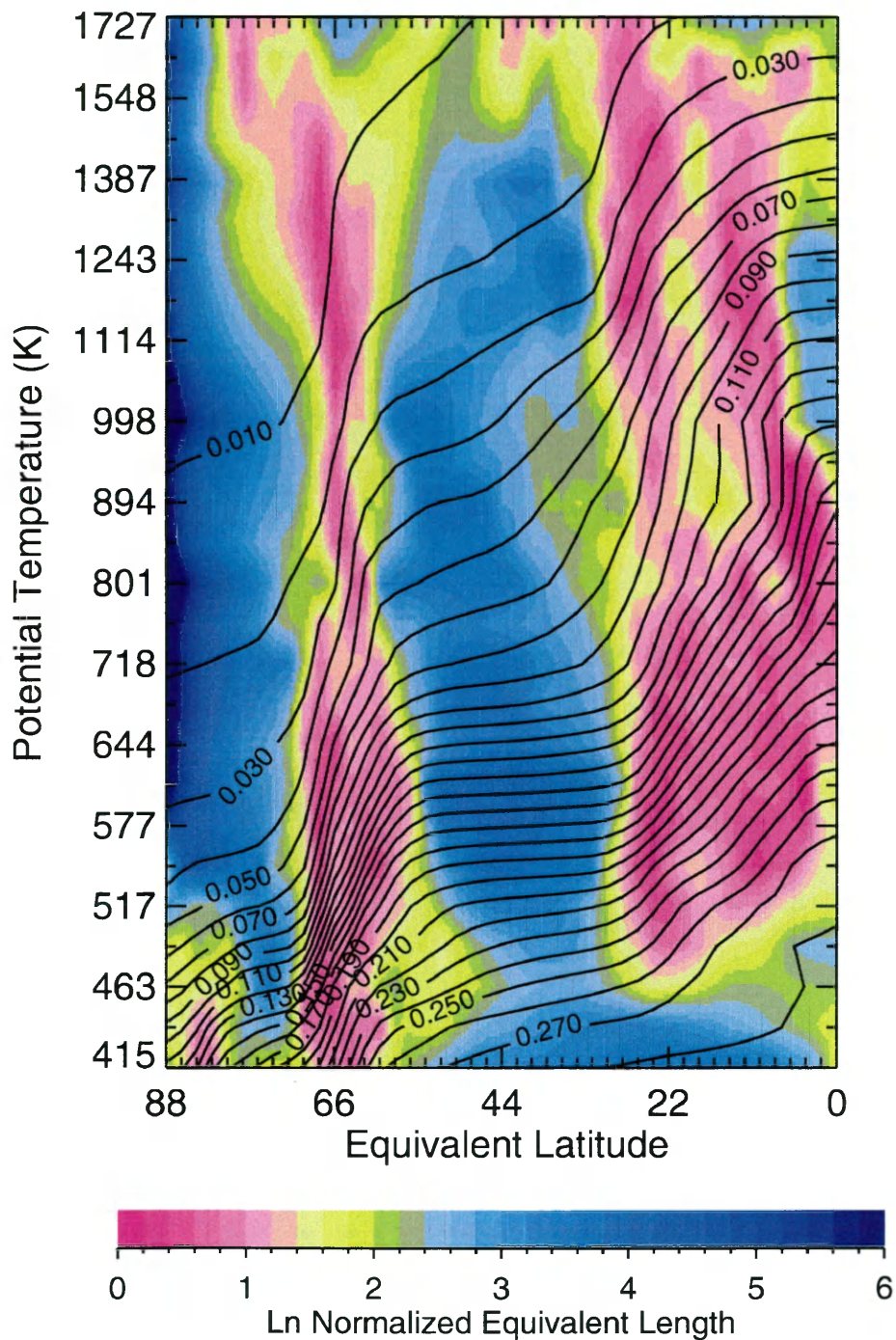


Figure 4.1. NMLM cross section of the CLAES northern hemisphere N₂O mixing ratio (ppmv, solid contours) and the natural log normalized equivalent length (color contours) sampled consistent with HALOE observations and then reconstructed using UKMO PV for February 13-19, 1993.

in the reconstructed data. At these levels, the magnitude of equivalent length for the reconstructed data agrees better with the gradient of the tracer mixing ratio. The NMLM analysis using the reconstructed N_2O data captures a more distinct polar vortex and a stronger surf zone (smaller equivalent lengths) than seen in the analysis using the actual CLAES data. This structure is most likely due to the influence of PV on the reconstructed data. In spite of these differences, it is concluded that the reconstructed data are a reasonable surrogate for the actual UARS data.

4.2 Reconstruction of Daily CH_4 Distributions and NMLM Results

HALOE CH_4 distributions were reconstructed following the outline in the previous section. Essentially, the PV versus CH_4 correlation on a discrete isentropic surface for the number of days required to obtain near-hemispheric coverage (~ 1 month) is used with the daily UKMO PV distribution to construct the CH_4 distribution for a specific day. Methane distributions are constructed for consecutive 7-day periods. The NMLM technique is then applied to the reconstructed HALOE CH_4 data. Averaging over 7-day time periods in the NMLM analysis improves the accuracy of the results by suppressing random noise in the data.

The NMLM results are analyzed using an area equivalent latitude versus potential temperature cross section of CH_4 mixing ratio and equivalent length. Figure 4.2, for example, shows NMLM results using HALOE CH_4 sunset data reconstructed from UKMO PV data. The PV versus CH_4 correlations on discrete isentropic surfaces were generated using data between April 15 and May 19, 1992. These correlations are then used with the UKMO PV data for each day to construct CH_4 distributions for

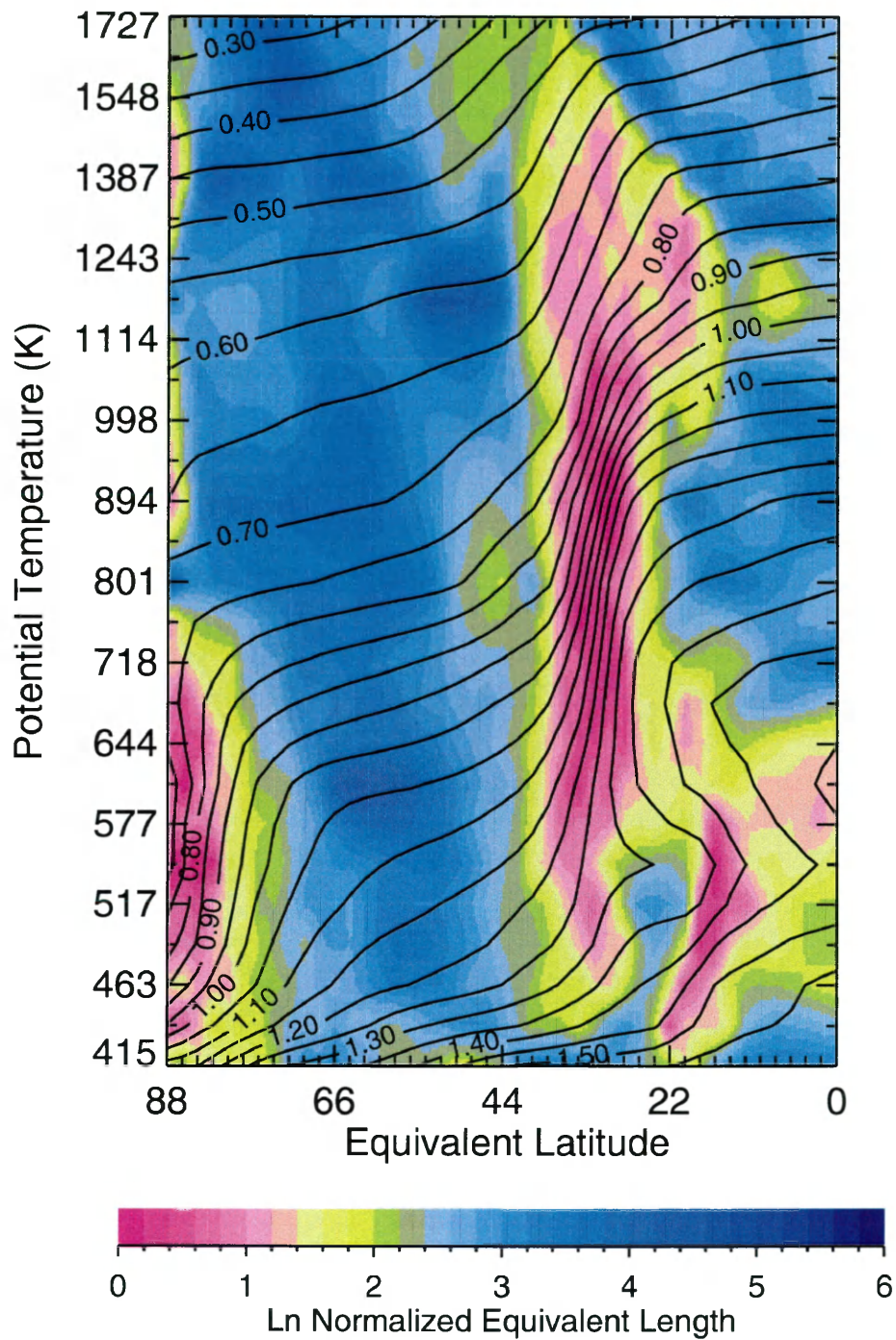


Figure 4.2. NMLM cross section of the northern hemisphere HALOE sunset CH₄ mixing ratio (ppmv, solid contours) and the natural log normalized equivalent length (color contours) reconstructed using UKMO PV for May 5-11, 1992.

May 5-11, 1992. The NMLM analysis of the reconstructed CH_4 data for this time period reveals interesting aspects of northern hemisphere springtime transport. The polar and subtropical barriers (i.e., regions of minimum equivalent length where meridional transport is restricted) are positioned at higher equivalent latitudes than seen in winter (see Figure 3.3). The polar vortex has disappeared in the middle and upper stratosphere above the 800 K isentropic surface as evidenced by the change from minimum to larger equivalent length, and quasi-horizontal mixing is enhanced in this region. During spring, the polar vortex is being destroyed by radiative processes, and the surf zone characterized by relatively large equivalent lengths and weak horizontal gradients (caused by repeated Rossby wave-breaking events) widens significantly.

4.3 Validity of the Approach

Since both CH_4 and N_2O are long-lived tracers and their distributions have a similar structure, the NMLM results using these species are expected to be very much alike. Therefore, application of the NMLM technique to solar occultation data was validated by comparing results obtained using the reconstructed HALOE CH_4 data with results obtained using CLAES N_2O data for the same periods. The results compare favorably. For example, the NMLM results using CLAES N_2O data for May 5-11, 1992, as shown in Figure 4.3, agree reasonably well with the results using reconstructed HALOE CH_4 data for the same time period (see Figure 4.2). Generally, there is very little difference in the positions and areas of small and large equivalent lengths. The large equivalent lengths seen in the lower stratosphere N_2O data are likely

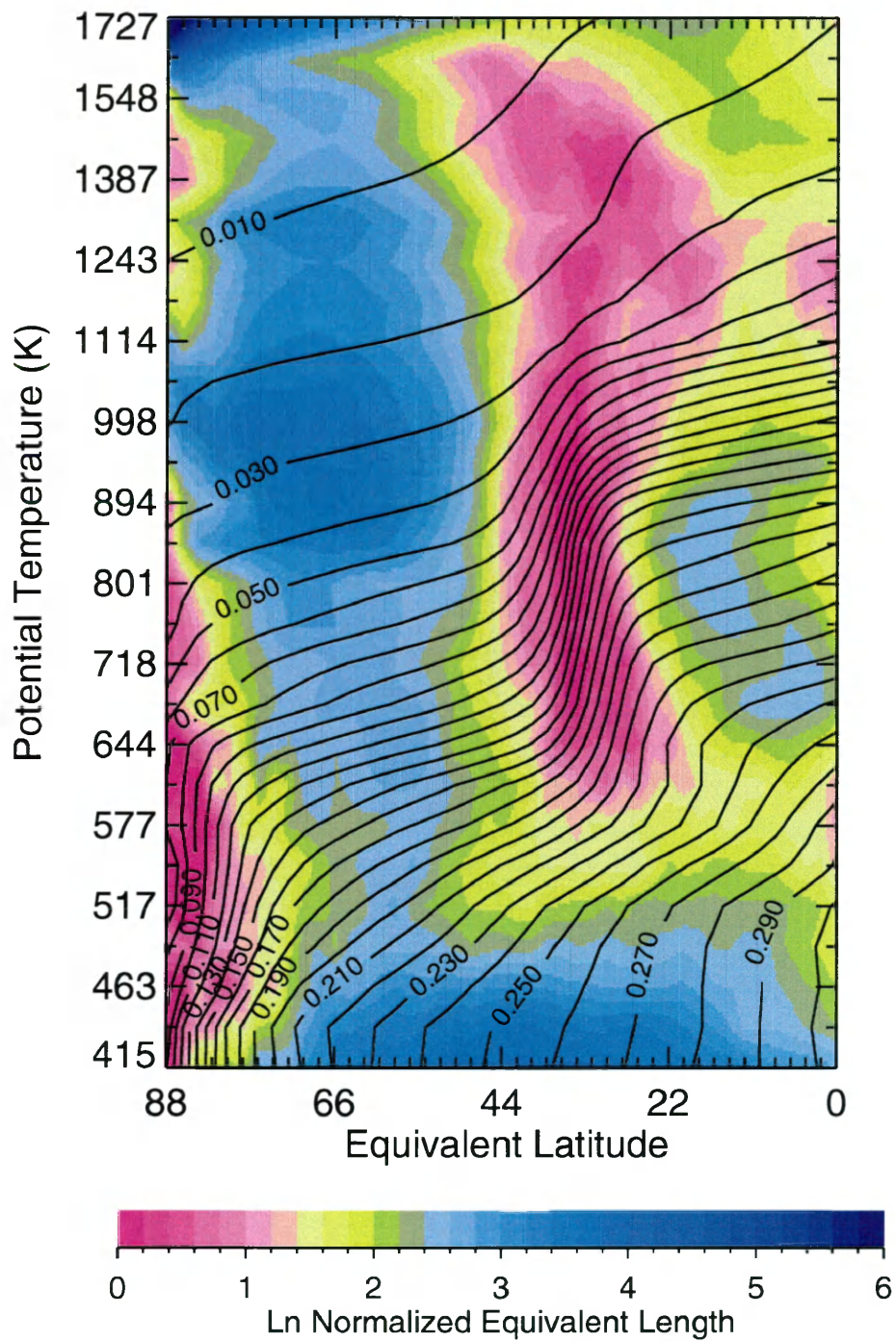


Figure 4.3. NLM cross section of the CLAES northern hemisphere N₂O mixing ratio (ppmv, solid contours) and the natural log normalized equivalent length (color contours) for May 5-11, 1992.

due to a CLAES aerosol contamination problem as mentioned by *Nakamura and Ma* [1997].

By exploiting the close relationship between PV and long-lived tracer distributions, reconstruction of HALOE CH₄ using PV is possible. However, the information that PV and CH₄ provide is not redundant, and both entities affect the NMLM analyses. This can be verified by first observing that the PV versus CH₄ correlations are not linear. If these correlations were linear then CH₄ would be contributing no new information, and the NMLM analysis using reconstructed CH₄ would merely reflect the PV distribution in CH₄ units. Figure 4.4 shows a typical correlation between PV and CH₄ and the average fit used in constructing the CH₄ fields. To complement the correlations and better identify the contributions of PV and CH₄, hemispheric distributions of PV and reconstructed CH₄ on isentropic surfaces were examined. They reveal that the synoptic structure of CH₄ is mainly determined by the PV distribution. However, the magnitude of the horizontal gradient is affected by CH₄. Polar stereographic maps of northern hemisphere PV and reconstructed CH₄ on the 801 K isentropic surface (~29 km) for May 5, 1992 are shown in Figure 4.5. The PV and CH₄ data are normalized by their corresponding maximum values for a one-to-one comparison. For each contour of CH₄ there is a similar contour of PV indicating that most of the hemispheric structure is that of PV. The pole-to-equator gradients for both entities are very inhomogeneous, with highly concentrated horizontal gradients between approximately 25-45° latitude. It can be seen that the magnitude of these variations is very much influenced by CH₄. Finally, results of the NMLM technique applied to the PV data, to the reconstructed CH₄ data, and to the

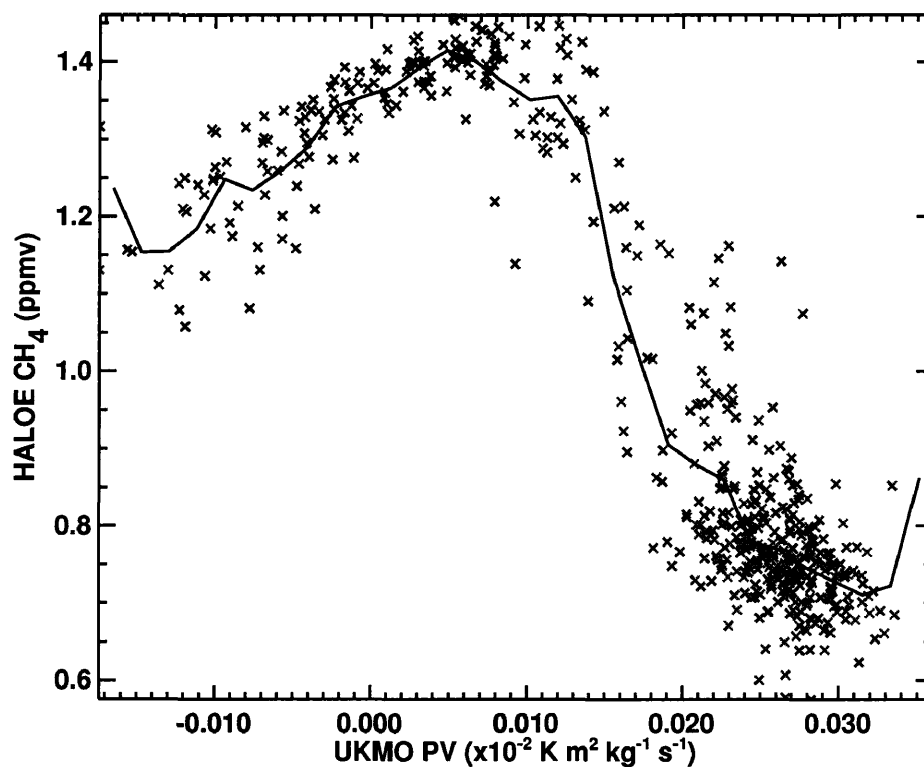


Figure 4.4. UKMO PV versus HALOE CH₄ correlation on the 801 K isentropic surface based on data from April 15 through May 19, 1992. Solid line is the average of the CH₄ data in PV bins. Negative PV values indicate southern hemisphere data.

CH₄ data spanning approximately one month are compared. The NMLM results using northern hemisphere PV data for May 5-11, 1992 are presented in Figure 4.6. The main differences in these results and the NMLM results using reconstructed CH₄ (see Figure 4.2) are observed in the subtropical barrier region (i.e., around 30° equivalent latitude). In this region the CH₄ horizontal gradients are compact (as seen in the hemispheric distributions), so that for a small change in the area enclosed by contours

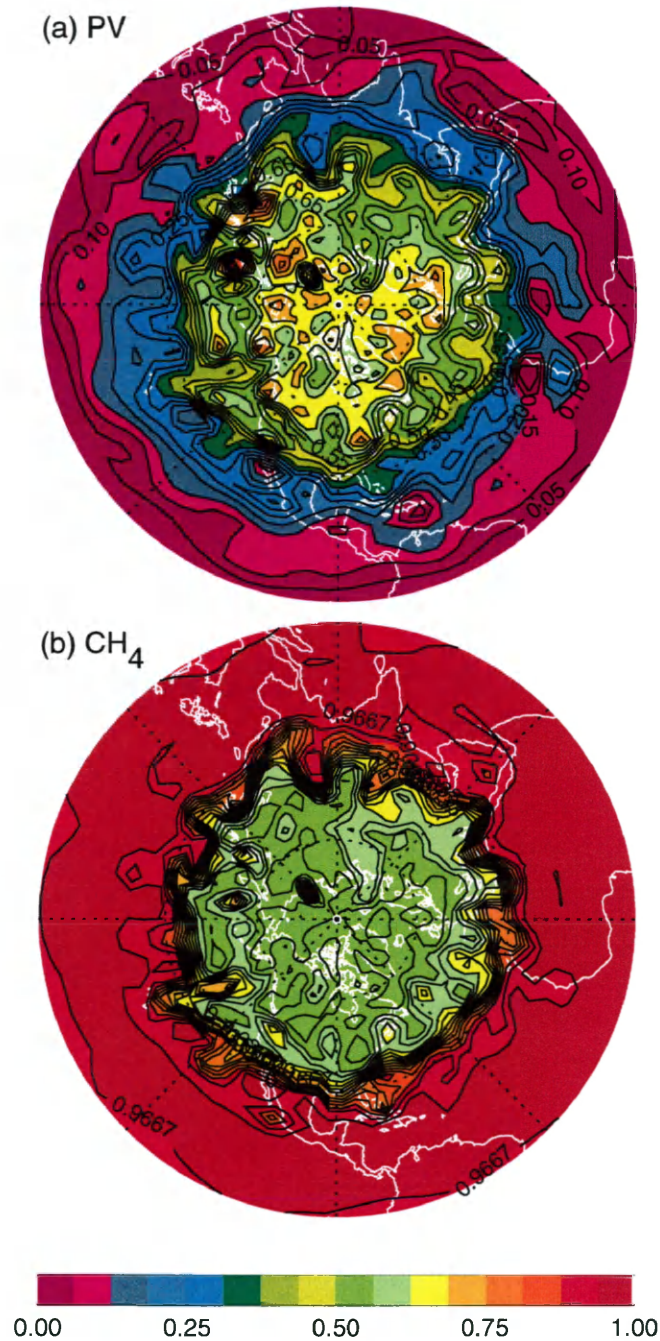


Figure 4.5. Polar stereographic map on the 801 K isentropic surface for May 5, 1992 of northern hemisphere (a) PV linearly interpolated to a $4^\circ \times 4^\circ$ latitude-longitude grid and to an evenly spaced $\ln(\theta)$ grid, and (b) HALOE CH₄ reconstructed using UKMO PV. PV and CH₄ values are normalized by their corresponding maximum values.

of constant CH_4 mixing ratio there is a relatively large change in the CH_4 value. This is reflected in the NMLM analysis as small equivalent lengths and sharp tracer edges, indicating a strong transport barrier. Potential vorticity has less of a horizontal gradient in this region and consequently shows a weaker and broader barrier. Figure 4.7 displays the NMLM results using northern hemisphere HALOE sunset CH_4 data spanning 35 days from April 15 to May 19, 1992. The strong subtropical barrier as well as the strong lower-level polar barrier visible in the reconstructed CH_4 results (see Figure 4.2) are evident in the month-long results. Since barriers of similar strength are not seen in the PV NMLM analysis (see Figure 4.6), this is a good indication that the CH_4 data very much influences the reconstructed CH_4 NMLM results.

Since near-hemispheric coverage exists daily for CLAES N_2O data, these data are used during an active northern hemisphere winter to determine the consequences of using long-term (~ 1 month) correlations to reconstruct synoptic hemispheric tracer distributions. The PV versus N_2O correlations on discrete isentropic surfaces were generated using data spanning two different time periods: (1) February 12 - March 16, 1993; and (2) February 13-19, 1993. These correlations were then used with the UKMO PV data for each day to construct N_2O distributions for February 13-19, 1993. The NMLM technique was applied to the reconstructed N_2O data for these two time periods, and the results were extremely similar. Because a dynamically active winter period was analyzed, the two NMLM results would be very different if the reconstructed N_2O distributions were affected by using a long-term correlation.

Based on the comparisons discussed in this section, we conclude that the NMLM formalism can be legitimately applied to solar occultation data provided a

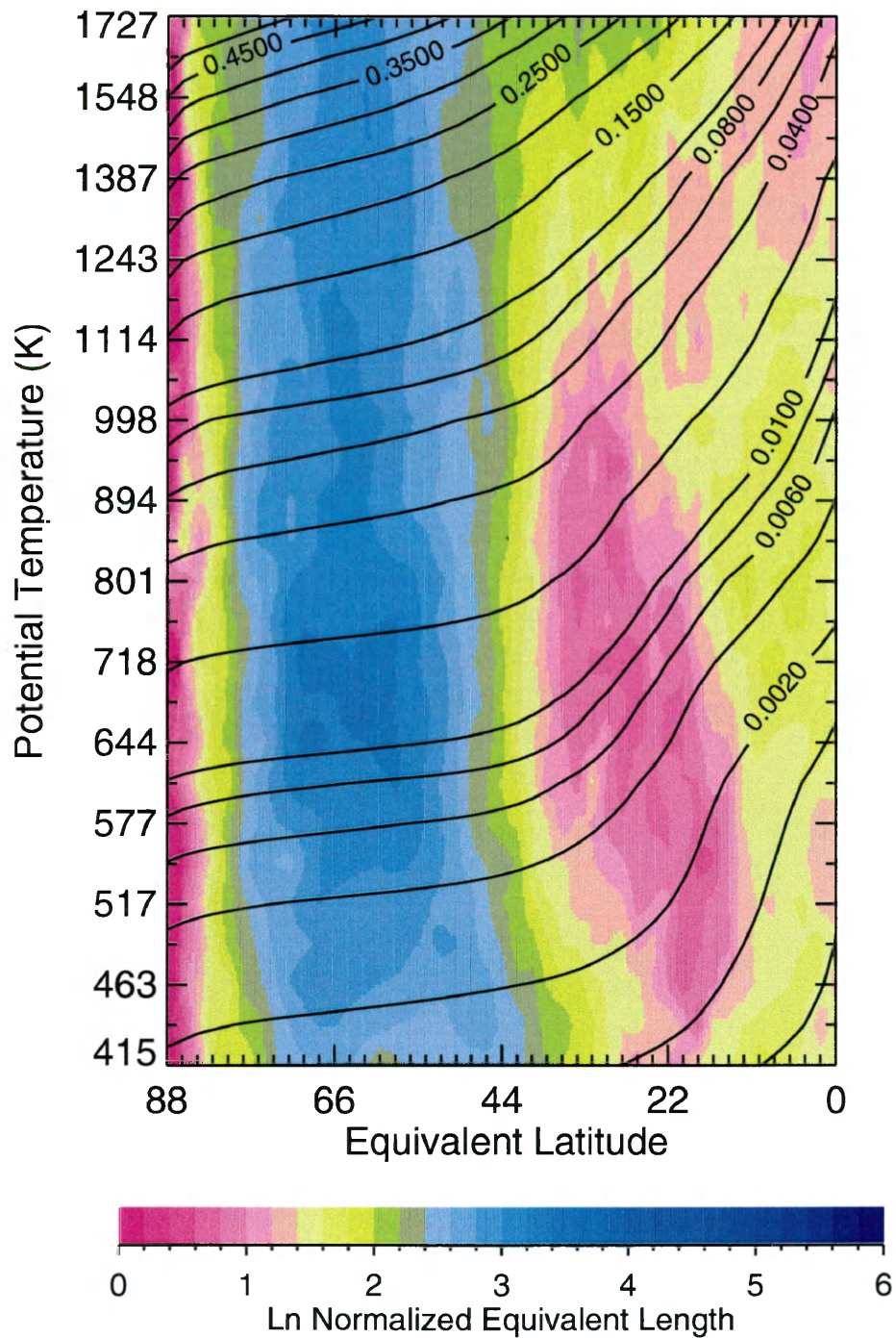


Figure 4.6. NMLM cross section of northern hemisphere PV ($\times 10^{-2} \text{ K m}^2 \text{ kg}^{-1} \text{ s}^{-1}$, solid contours) and the natural log normalized equivalent length (color contours) linearly interpolated to a $4^\circ \times 4^\circ$ latitude-longitude grid and to an evenly spaced $\ln(\theta)$ grid for May 5-11, 1992.

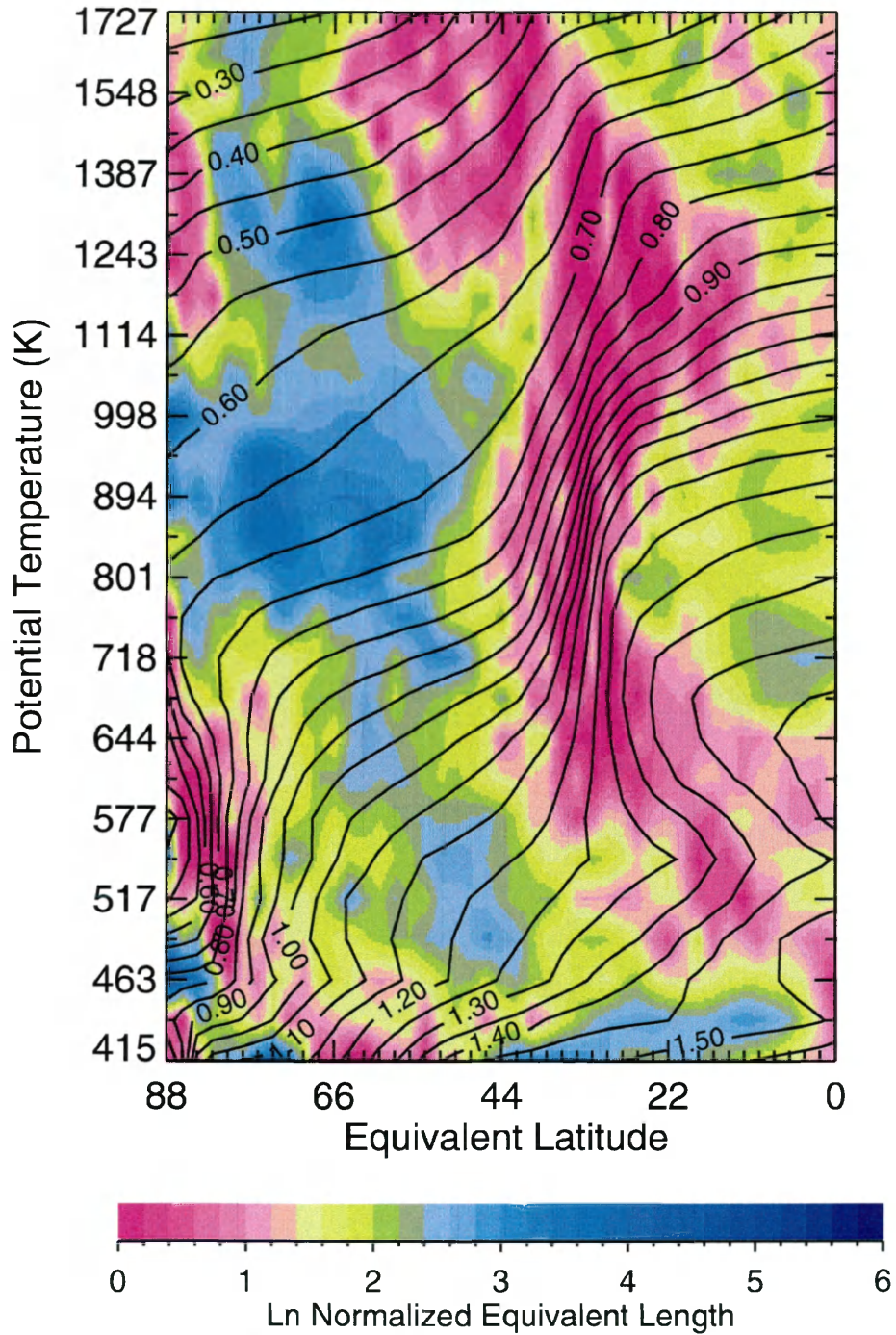


Figure 4.7. NMLM cross section of the northern hemisphere HALOE sunset CH₄ mixing ratio (ppmv, solid contours) and the natural log normalized equivalent length (color contours) for April 15 through May 19, 1992.

suitable synoptic distribution of PV can be obtained for the desired period. The reconstruction technique appears capable of resolving features of the tracer as well as PV.

CHAPTER V

TRACER CORRELATIONS

The primary goal of this research is to examine transport in the lower stratosphere. This chapter illustrates efforts to utilize the synergy between aircraft and satellite data to meet this goal. The in situ ER-2 measurements provide data that are higher in resolution, precision, and accuracy than are satellite data. Unfortunately, these data have limited spatial and temporal coverage and are unable to resolve large-scale transport issues. The remote observations from the HALOE instrument supplement the ER-2 observations by providing a more global perspective at the expense of lower resolution, precision, and accuracy than the aircraft data. The measurement characteristics of the ER-2 and HALOE instruments, and the precision and accuracy of the data sets were discussed in Chapter 2.

Tracer correlations are used in the following scenario. First, correlations based upon HALOE measurements are compared with those from the ER-2 to assess the satellite data. The very good agreement achieved between the ER-2 and HALOE CH₄ versus O₃ correlations increased our confidence in using the HALOE CH₄ data in global NMLM analyses. Then, ER-2 tracer correlations are examined in conjunction with coincident HALOE NMLM results. This provides for a less ambiguous interpretation of the correlations and a more balanced approach in studying transport.

5.1 Comparison of Aircraft and Satellite Tracer Correlations

ER-2 and HALOE data were examined for time periods that coincide with ER-2 flights covering five aircraft campaigns from 1991 through 1997. The CH_4 versus O_3 correlations were obtained for both ER-2 and HALOE data spanning specific time periods and binned in potential temperature ranging from 350 to 550 K (~14-22 km). To compare with the ER-2 correlations, the HALOE observations were restricted in latitude and longitude corresponding to the ER-2 ranges and combined over a time range of two weeks or less around the ER-2 flight days.

The ER-2 and HALOE correlations for northern hemisphere 1991 fall and 1992 winter were in poor agreement. During this time period the HALOE data in the lower stratosphere are most likely contaminated with aerosol due to the Mount Pinatubo volcanic eruption in June 1991, and in many cases, the HALOE observations were too sparse to achieve a valid comparison with the ER-2 correlations.

The agreement between the ER-2 and HALOE correlations for 1993 through 1997 is mainly very good. During the five year time span both hemispheres and a variety of seasons were sampled. In general the CH_4 versus O_3 correlations for the ER-2 and HALOE data overlap on isentropic surfaces. A typical comparison is shown in Figure 5.1 for isentropic surfaces ranging from 410 to 450 K every 10 K. These data were obtained in the 1994 southern hemisphere spring between 40° and 70° latitude and between 147° and 195° east longitude. The HALOE CH_4 versus O_3 correlations, that include observations for October 3-20, have the same structure as the ER-2 correlations that span seven flights (October 3,5,8,10,13,16,20) during the ASHOE/MAESA campaign. Good agreement also exists for the entire vertical extent

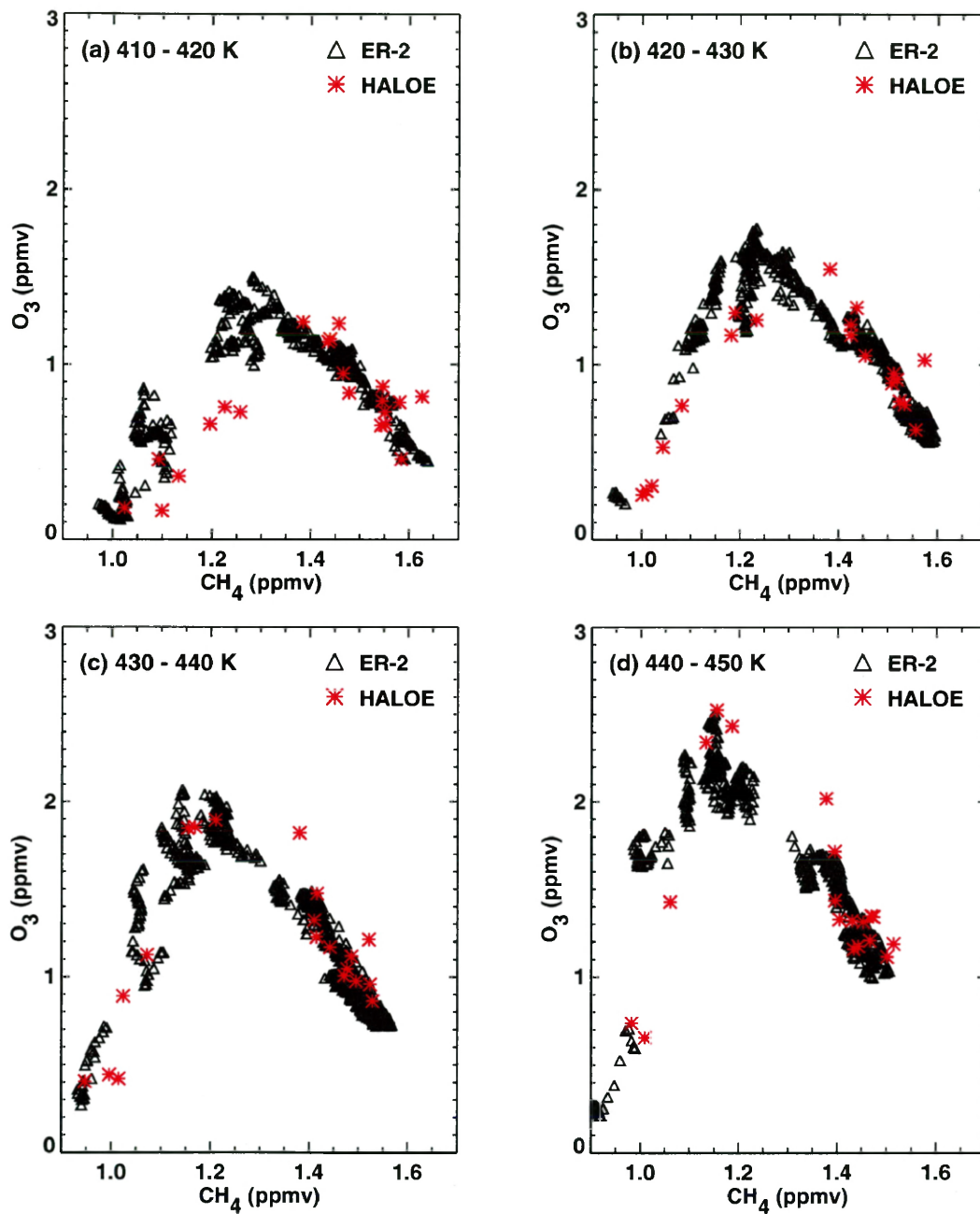


Figure 5.1. CH_4 versus O_3 correlations for October 3-20, 1994 ranging in latitude between 43° and 70° south, ranging in longitude between 147° and 195° east, and covering four potential temperature ranges. Black triangles identify ER-2 data for six flights and red stars identify HALOE sunset data.

of the observations as illustrated in Figure 5.2. In this figure, the CH₄ versus O₃ correlations include data ranging in latitude from 61° to 85° north, ranging in longitude from 203° to 258° east, and covering a potential temperature range from 350 to 550 K. The HALOE correlation includes observations for May 6-20, 1997, and the ER-2 correlation consists of data from four flights (May 6,9,11,13) during the POLARIS campaign. Some outliers are evident in both the ER-2 and HALOE correlations, but most of the HALOE points overlap the ER-2 measurements.

Reasonable agreement between the ER-2 and HALOE correlations establishes the feasibility of using these complementary measurements from aircraft and satellite platforms to facilitate transport studies in the lower stratosphere. Good agreement between the ER-2 and HALOE correlations indicates that HALOE data in the lower stratosphere can be used confidently in global analyses. The correlation comparisons are especially useful at altitudes below the 100 mbar level (i.e., below ~16 km or for isentropic surfaces less than ~450 K) where the estimated errors in the HALOE data are not well known (see Figure 5.1).

5.2 Analysis Using ER-2 Tracer Correlations and HALOE NMLM Results

As mentioned in Chapter 1, correlations between tracer data obtained during aircraft campaigns have been used extensively to deduce transport and mixing as well as chemical processes occurring in the lower stratosphere. However, interpretation of what the tracer correlations show without ancillary information can be ambiguous at times due to the competition between various atmospheric processes (e.g., isentropic mixing, vertical advection, chemical loss) that can change tracer distributions.

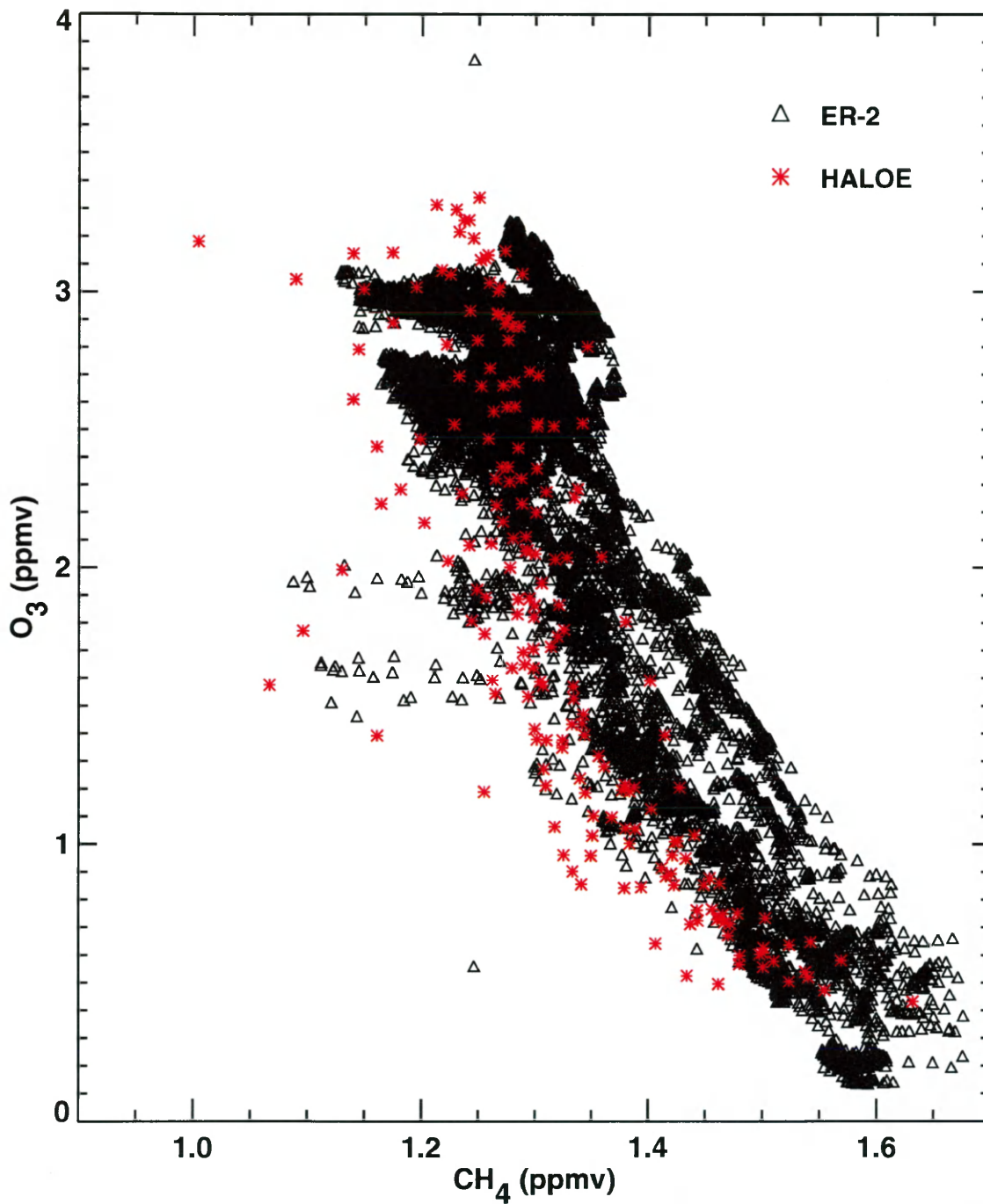


Figure 5.2. CH₄ versus O₃ correlation for May 6-20, 1997 ranging in latitude between 61° and 85° north, ranging in longitude between 203° and 258° east, and covering a potential temperature range from 350 to 550 K. Black triangles identify ER-2 data for four flights and red stars identify HALOE sunrise data.

In the meridional plane [Holton, 1986a,b; Mahlman *et al.*, 1986], the distributions of long-lived stratospheric tracers have mixing ratio isopleths that bulge upward in the tropics and slope poleward and downward relative to the isentropic surfaces. Vertical transport by the mean meridional cell tends to steepen the slopes of the tracer mixing ratio surfaces. At mid- to high-latitudes in the winter hemisphere isentropic mixing tends to flatten the tracer isopleths. Also, chemical loss or production can have a slope flattening effect. When two tracers have isopleths that are parallel to each other and have similar horizontal and vertical gradients, they are in slope equilibrium and gradient equilibrium, and their mixing ratios display a linear, compact relationship [Plumb and Ko, 1992]. In general, long-lived tracers exhibit correlations that may differ from the linear, compact relationship of idealized tracers [Murphy *et al.*, 1993; Plumb, 1996]. The departure from a compact relationship in tracer correlations could be due to (1) species having very different chemical loss or production rates or relative short local lifetimes; (2) spatial and temporal variability in horizontal and/or vertical transport that result in inhomogeneous mixing of different air masses; or (3) measurement uncertainties, and is subject to individual analysis. Therefore, separating the effects of chemistry and transport by interpreting tracer correlations is a major challenge, and associating ER-2 tracer correlations with HALOE NMLM results should provide for a less ambiguous interpretation of the correlation diagrams. The CH₄ versus O₃ correlation shown in Figure 5.3 does not reveal a compact mutual relationship, and both negative and positive slopes or scatter exists for most of the potential temperature ranges. The data include ER-2 measurements during the 1994 austral (southern) spring on three flights (October

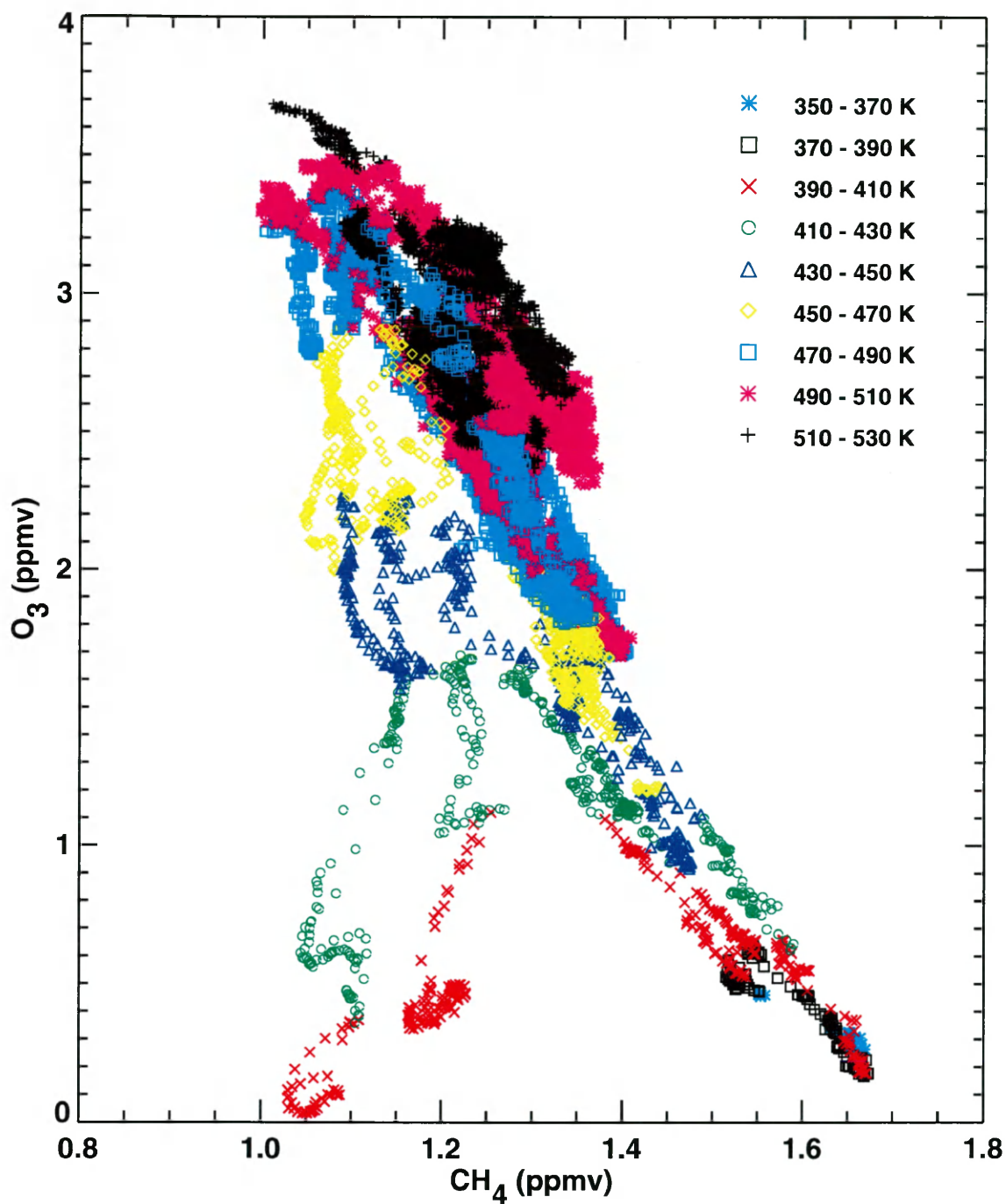


Figure 5.3. ER-2 CH₄ versus O₃ correlation for October 10,13,16, 1994 ranging in latitude between 43° and 70° south, ranging in longitude between 171° and 182° east, and covering a potential temperature range from 350 to 530 K.

10,13,16) and span 43° to 70° in latitude, 171° to 182° east in longitude, and 350 to 530 K in potential temperature (~ 14 -21 km). Examining the CH_4 versus O_3 correlation diagram with these data sorted by latitude instead of potential temperature shows that the positive slopes and scatter seen in Figure 5.3 occur at latitudes poleward of 67° south only. The scatterplot of CH_4 versus O_3 collapses to a nearly compact curve with a negative slope if data at these latitudes are excluded. Even though, in the polar region during austral spring, chemical destruction of O_3 is the most likely mechanism responsible for the anomalies, it is not clear from the scatterplots alone whether the departures from a single compact curve is primarily a result of chemistry or dynamics.

To aid in the interpretation of Figure 5.3, NMLM results were generated using reconstructed HALOE CH_4 data. The UKMO PV versus HALOE CH_4 correlations, which included data from October 3 to November 6, 1994, and the daily PV fields were used to reconstruct synoptic, southern hemisphere CH_4 distributions for October 9-15, 1994. The results of applying the NMLM technique to these reconstructed CH_4 data is shown in Figure 5.4. Between 43° and 70° south latitude, where the ER-2 in situ measurements were obtained, the NMLM analysis shows three distinct regions: a surf zone, a barrier region centered around 60° equivalent latitude, and a polar region. The barrier region separates the polar region from the midlatitude surf zone vertically throughout the lower stratosphere and increases its latitudinal extent with altitude. On isentropic surfaces above approximately 390 K this barrier strongly restricts lateral transport (minimal equivalent length accompanied by sharp horizontal tracer gradients). As a result, the air in the polar region of the lower stratosphere is

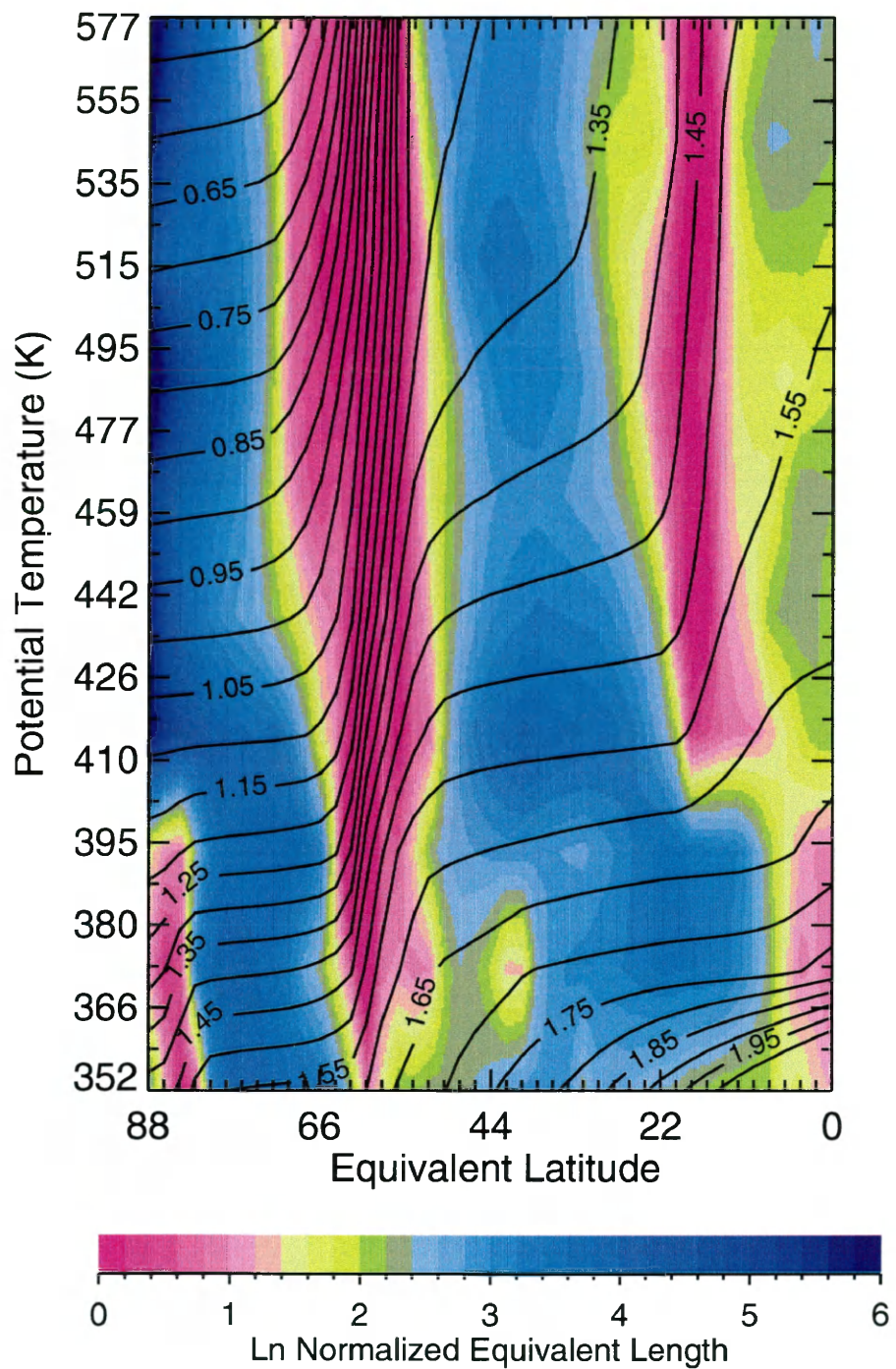


Figure 5.4. NMLM cross section of the southern hemisphere HALOE sunset CH₄ mixing ratio (ppmv, solid contours) and the natural log normalized equivalent length (color contours) reconstructed using UKMO PV for October 9-15, 1994.

essentially isolated from the lower-latitude air.

At latitudes between 67° and 70° south where deviations from a compact correlation curve occur, the observations are either in the polar region or on the poleward side of the barrier region. The observations that fall completely in the polar region are on isentropic surfaces between 390 and 430 K. In Figure 5.3 the observations on the 390-410 K and 410-430 K isentropic surfaces are plotted as red and green points, respectively. An interesting feature of the observations on these surfaces are the discontinuous correlation curves. The correlation curve has a negative slope occurring at latitudes between 43° and 46° south that reverses to a positive slope at latitudes between 67° and 70° south. The NMLM analysis (see Figure 5.4) shows that this discontinuity is due to sampling two distinct air masses that are separated by the dynamical barrier to mixing. On the surf zone side of this barrier rapid quasi-horizontal mixing results in correlations forming a negative slope. On the polar side of the barrier, air experiences prolonged periods of isolation and mixing of air masses from above produce another slope (positive).

On isentropic surfaces above 430 K, the CH_4 versus O_3 correlation consists of negatively sloping, compact curves that become diffuse on all surfaces for observations obtained in the 67° - 70° south latitude range (see Figure 5.3). Referring to the NMLM analysis, these measurements occurred on the poleward side of the barrier. Methane and ozone being uncorrelated in this region strongly implies chemical changes in O_3 . If this lack of correlation was purely a result of vertical descent of O_3 then transport would also bring down low CH_4 . Between 67° and 70° latitude, the tracer scatterplot displays a minimum CH_4 mixing ratio of 1 part per

million by volume (ppmv) and O_3 mixing ratios less than approximately 3 ppmv. Descent of O_3 with concentrations of 3 ppmv or less would require transport of air from the upper stratosphere where the abundance of CH_4 is only a few tenths of a ppmv. Thus, the higher CH_4 observed suggests that vertical descent is not the sole cause of scatter in this region. Similarly, the positive slopes observed inside the polar vortex below the 430 K surface suggests that O_3 is being chemically destroyed since CH_4 decreases and typically O_3 increases with altitude in the lower stratosphere.

The NMLM technique is strictly a transport oriented analysis. Implementing this technique using observations of any passive tracer will clearly identify quasi-horizontal transport barriers and mixing regions. Tracer correlations, on the other hand, include the effects of both chemistry and transport. Therefore, in order to assess the usefulness of correlations in deducing lateral transport, the NMLM analysis and tracer correlation must cover spatial areas that are experiencing no chemical processing and minimal vertical descent, for example the subtropical region. To facilitate this assessment, an ER-2 CH_4 versus O_3 correlation and an NMLM analysis were evaluated between 14° and 38° north latitude in the lower stratosphere during spring when one would expect little or no effects of chemistry on either CH_4 or O_3 .

An ER-2 CH_4 and O_3 correlation, based on northern hemisphere measurements on May 3, 1993, is plotted in Figure 5.5. The observations are sorted by potential temperature, and only data on isentropic surfaces above 410 K are analyzed to guarantee that only stratospheric air masses are included in the correlation. The scatterplot indicates that CH_4 and O_3 are not in perfect slope equilibrium whose relationship is represented by a single compact curve. Instead, there is an obvious

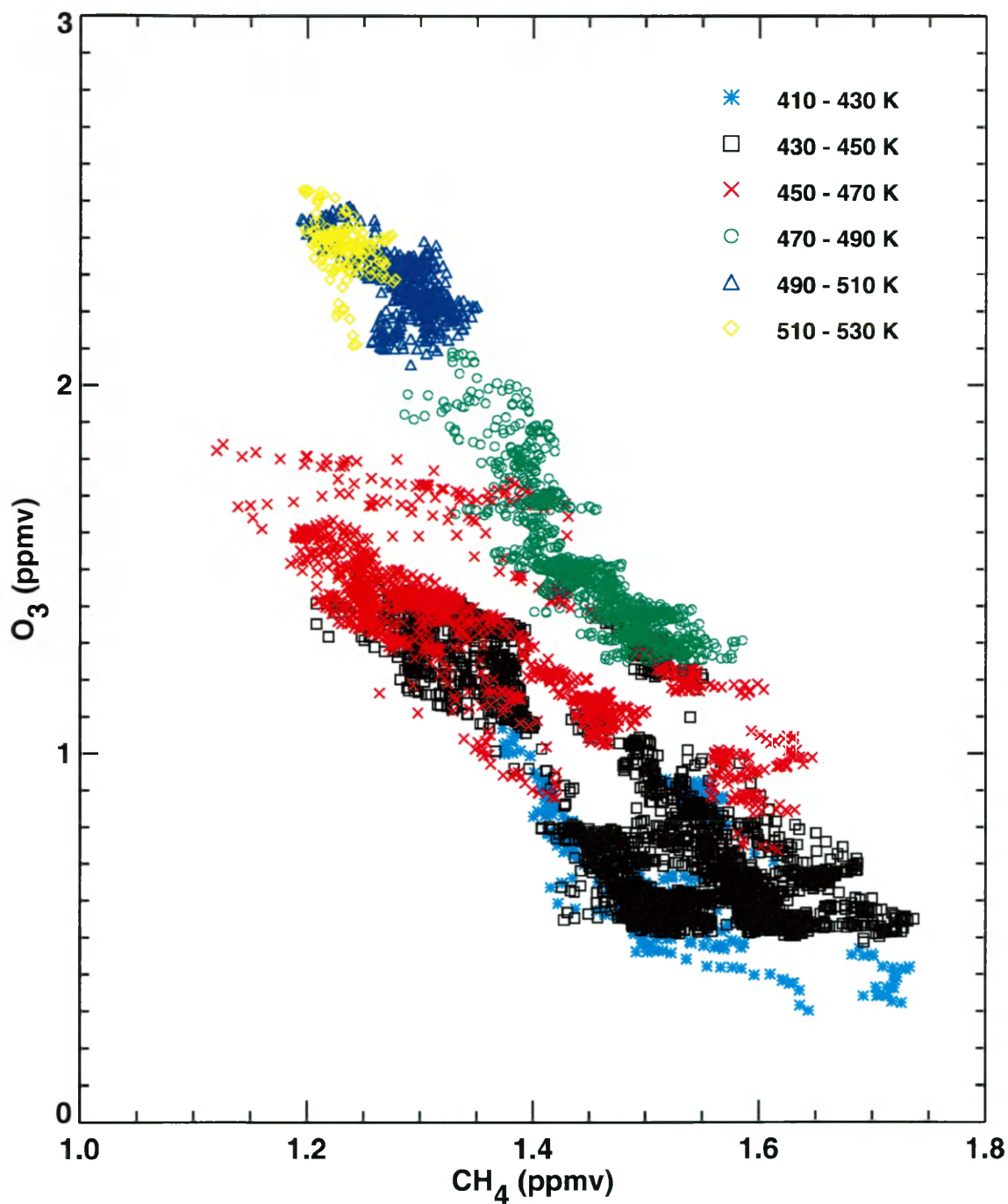


Figure 5.5. ER-2 CH₄ versus O₃ correlation for May 3, 1993 ranging in latitude between 14° and 38° north, ranging in longitude between 237° and 243° east, and covering a potential temperature range from 410 to 530 K.

discontinuity between the correlations above and below the 470 K isentropic surface. A compact tracer correlation with a negative slope exists for observations obtained on surfaces above 470 K, however on surfaces below 470 K, the correlation shows considerable scatter. The presence of scatter in the correlation of tracers experiencing no chemical processing or vertical descent could be an indication of inefficient mixing. Examination of the coincident NMLM analysis appears to support an anomalous mixing scenario.

Figure 5.6 displays the NMLM cross section of northern hemisphere HALOE CH_4 reconstructed using UKMO PV versus HALOE CH_4 correlations, that included April 10 through May 14, 1993 data, and the daily PV data from April 27 to May 3, 1993. Within the region of interest (i.e., between 14° and 38° latitude and between 410 and 530 K isentropic surfaces), a subtropical barrier separates the midlatitude surf zone from the tropical region in the lower stratosphere on surfaces above approximately 430 K. This barrier is centered around 23° equivalent latitude and increases not only its latitudinal extent with altitude but also its strength. The scatter observed in the CH_4 versus O_3 correlation is directly influenced by the strength of the subtropical barrier. On isentropic surfaces below 470 K, quasi-horizontal transport is only weakly inhibited. Transport is more restricted on surfaces above 470 K (i.e., smaller equivalent lengths and more concentrated horizontal tracer gradients). This follows a study by *Waugh* [1996] that showed in the northern hemisphere during the fall to spring period (late September to early May) transport out of the tropics in the lower stratosphere is greater around the 425 K isentropic surface than near the 500 K surface. Air transported out of the tropics on surfaces between 410 and 470 K does not

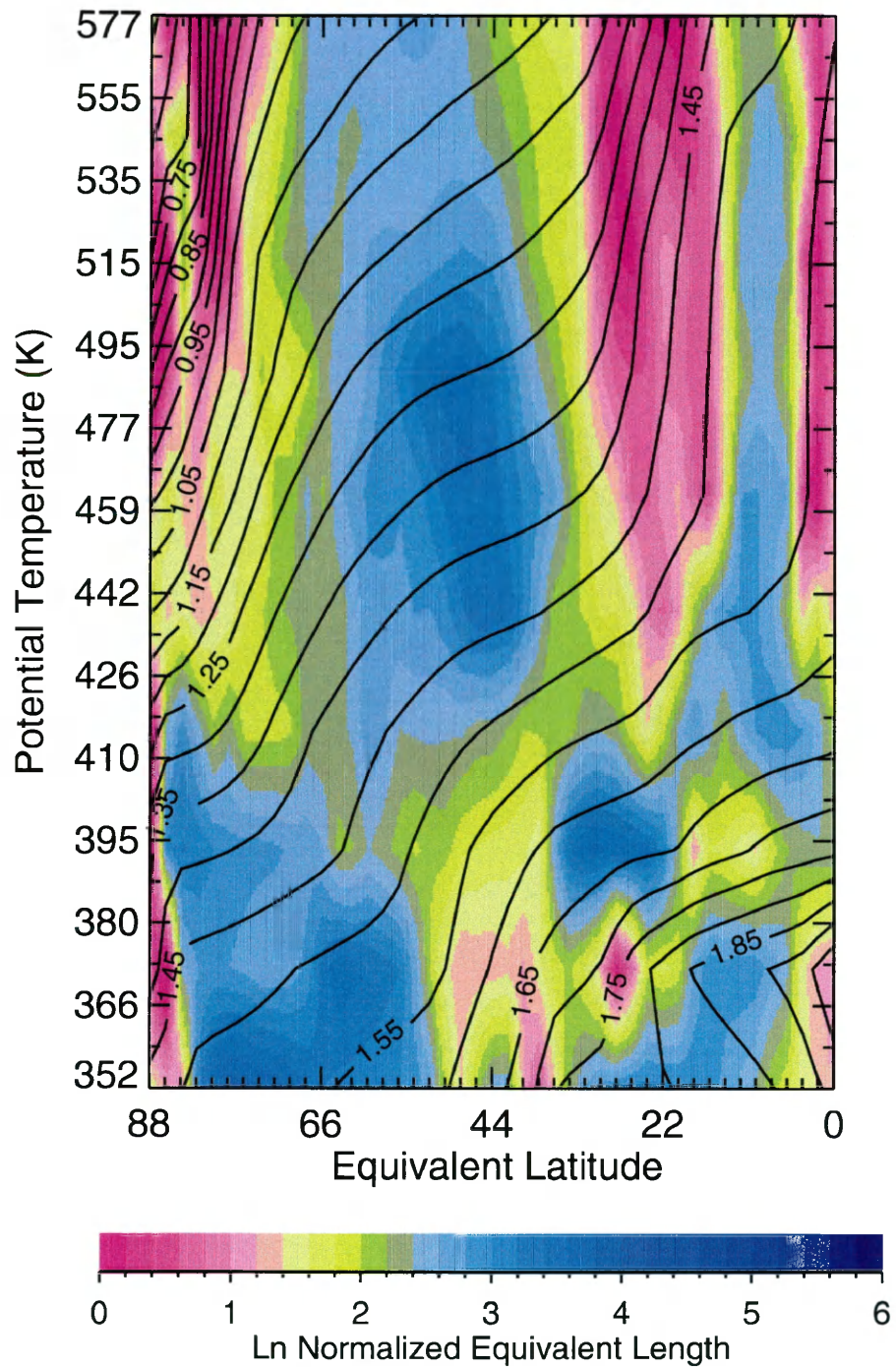


Figure 5.6. NMLM cross section of the northern hemisphere HALOE sunset CH₄ mixing ratio (ppmv, solid contours) and the natural log normalized equivalent length (color contours) reconstructed using UKMO PV for April 27-May 3, 1993.

undergo vigorous quasi-horizontal mixing in the latitude region sampled by the ER-2 instruments (see subtropical yellow and pink areas in Figure 5.6). As a result, the tropical and extratropical air masses are not homogenized, and the tracer correlation reveals a significant amount of scatter in this region. Transport out of the tropical region is insignificant in the well-correlated region above the 470 K isentropic surface.

Tracer correlations have been coupled with other analyses, such as contour advection [*Waugh et al.*, 1997] and trajectory mapping [*Pierce et al.*, 1997] techniques, to evaluate the influence of chemistry and dynamics on observations. Using tracer correlations in conjunction with the NMLM analyses gives yet another perspective for evaluating the role of lateral transport on stratospheric measurements. The advantages of this procedure are a less ambiguous interpretation of the tracer correlations and both a small-scale and large-scale approach in studying transport. However, to make the most of these tools, knowing the chemical and dynamical characteristics of the species and stratosphere, respectively, is absolutely essential.

CHAPTER VI

SUMMARY AND CONCLUSIONS

Transport characteristics of the lower stratosphere were examined by utilizing tracer correlations based upon aircraft data in conjunction with a modified Lagrangian-mean analysis using satellite occultation data. Coupling these analyses (and data sets) provides for a more comprehensive interpretation of the observations and a more balanced approach in studying transport.

A very important aspect of this work involved implementing the modified Lagrangian-mean technique developed by Nakamura [Nakamura, 1995, 1996, 1998; Nakamura and Ma, 1997; Nakamura *et al.*, 1999] using occultation data. This technique allows deduction of certain aspects of the transport characteristics knowing only the mixing ratio of long-lived tracers. The method easily identifies so-called transport barriers or regions where quasi-horizontal transport is restricted. Potential temperature is used as the vertical coordinate and area enclosed by contours of constant mixing ratio on isentropic surfaces is used as the meridional coordinate. The NMLM technique can be applied to any long-lived tracer provided adequate spatial coverage can be achieved over a short period of time, that is, the characteristic time over which flow can be considered isentropic (~7-10 days in the lower stratosphere).

The NMLM formalism assumes that the cross-isentropic component of

transport is much slower than the component on isentropic surfaces (~ 1 week) and can be neglected, and that long-lived tracer distributions are determined by transport (i.e., chemical source and sink terms are neglected). Also, winds are assumed to be nondivergent on isentropic surfaces. Following the formal approach of Nakamura, the tracer transport equation is transformed to an area coordinate. First, the tracer mixing ratio is associated with the area its contour encloses on the isentropic surface. Due to the one-to-one relationship between area and tracer mixing ratio, a transport equation in the area coordinate is derived. A key NMLM diagnostic included in this equation is the equivalent length. It measures the efficiency of irreversible transport (i.e., isentropic mixing). Physically, equivalent length is the approximate perimeter length of the tracer contour enclosing an area. These contours can be severely deformed and may even enclose areas separated from the main entity. A large equivalent length indicates substantial stretching of the tracer contour which is associated with rapid quasi-horizontal transport and mixing. A small equivalent length identifies regions where meridional transport is restricted. The NMLM results (i.e., tracer mixing ratio and equivalent length) are displayed (and analyzed) as area equivalent latitude versus potential temperature cross sections.

Nakamura applied his technique using CLAES N_2O data. The CLAES instrument is a limb sounder and obtains near-hemispheric coverage each day. Unfortunately, the CLAES data only extend from October 1991 to May 1993. In this research, HALOE CH_4 observations which provide eight years of data from October 1991 to the present are used. However, the solar occultation sampling pattern of HALOE requires approximately one month to obtain near-hemispheric coverage, and

assuming isentropic flow over this time period may not be valid. Consequently, by exploiting the close relationship between potential vorticity and long-lived tracers, synoptic hemispheric CH₄ distributions are constructed using daily PV distributions. For each isentropic surface, a UKMO PV versus HALOE CH₄ correlation is obtained and includes data for all days required to get near-hemispheric coverage (~1 month for HALOE data). Using this correlation along with the daily PV distribution, HALOE CH₄ is constructed for a specific day. The NMLM technique is then applied to the reconstructed HALOE CH₄ data and for 7-day periods to suppress random noise in the data.

The information provided by PV and CH₄ in the reconstructed distributions is not redundant, and both entities affect the NMLM analyses. We observed that the PV versus CH₄ correlations are not linear, and therefore CH₄ is contributing new information and not merely reflecting the PV distribution. Hemispheric distributions of PV and reconstructed CH₄ on isentropic surfaces were also examined. They showed that PV significantly influences the synoptic structure of CH₄, and CH₄ influences the magnitude of the horizontal gradient. Finally, the NMLM technique is applied to PV distributions and to HALOE CH₄ data spanning 35 days (time required to achieve near-hemispheric coverage). These results were compared with the NMLM analysis using the reconstructed HALOE CH₄ data. The comparison confirmed what was concluded from the hemispheric distributions of PV and reconstructed CH₄ (i.e., PV affects the CH₄ structure and CH₄ affects the horizontal gradient).

Ultimately, we demonstrated that it is feasible to apply the NMLM technique to solar occultation data when used in conjunction with daily PV distributions to

identify lateral transport barriers and mixing regions. Application of the NMLM technique to solar occultation data was validated by comparing results obtained using the reconstructed HALOE CH₄ data with CLAES N₂O data for the same periods. Since CH₄ and N₂O are long-lived tracers with similar distributions, their NMLM results are expected to be much the same. And in fact the results compare favorably. For example, the NMLM analyses using reconstructed HALOE CH₄ data and CLAES N₂O data for May 5-11, 1992 show excellent agreement for the equivalent latitude location of both the polar and subtropical barriers. Also, there are very little differences in the areas of small and large equivalent lengths in the two analyses.

Tracer correlations are frequently the choice for interpreting the localized ER-2 aircraft measurements. However, unlike the NMLM analysis, correlations include the effects of both chemistry and transport. Separating these effects by merely examining tracer correlations is difficult and often ambiguous. A foreknowledge of chemical and dynamical processes that could influence the correlation is essential. An additional insight as to how the relationship between two tracers is affected by quasi-horizontal transport becomes evident when the correlation is associated with a coincident NMLM analysis.

Following the theory of *Plumb and Ko* [1992], a compact relationship is expected between long-lived tracers as a result of a balance between transport and chemical processes. A breakdown of this compact relationship and what is seen as scatter in correlation diagrams can be attributed to tracers having very different chemical loss or production rates or relative short local lifetimes, spatial and temporal variability in horizontal and/or vertical transport that result in inhomogeneous mixing

of different air masses, or measurement uncertainties. We demonstrate how scatter can be interpreted as chemical anomalies when the NMLM analysis indicates that lateral transport is inhibited and when vertical descent is ruled out based on the time evolution of the observed tracer concentrations. For example, CH_4 versus O_3 correlations and NMLM results using reconstructed HALOE CH_4 data were examined for a chemically active period (i.e., southern hemisphere spring). The NMLM analysis showed a strong polar barrier to lateral transport, isolating polar air from midlatitude air. Tracer correlations over the same time period exhibited a compact relationship forming a negative slope for air sampled on the surf zone side of the polar barrier, where rapid quasi-horizontal mixing efficiently homogenizes the air. However, the compact correlation curves become diffuse or discontinuous (forming a positive slope) for regions on the polar side of the transport barrier, where the air most likely reflects chemical processing. Also by examining a complementary NMLM cross section, we demonstrate that the presence of scatter in the tracer correlation in regions without significant local chemical activity or vertical descent is a direct indicator of anomalous mixing (i.e., slow quasi-horizontal transport and inefficient mixing of air masses). For this case, CH_4 and O_3 correlations and NMLM results using reconstructed HALOE CH_4 were examined in the subtropical region during northern hemisphere spring, where little or no effects of chemistry are expected on either CH_4 or O_3 . The NMLM analysis showed a subtropical barrier to lateral transport on isentropic surfaces above approximately 430 K. The strength of this barrier increased with altitude and directly influenced the tracer correlations. Tracer correlations exhibited a compact, negative-sloping relationship on surfaces above 470 K, where the subtropical barrier is relative

strong and thus isolates tropical and extratropical air. The air sampled on these surfaces is from the surf zone side of the barrier and is well mixed. On isentropic surfaces below 470 K, tracer correlations were diffuse. Here the NMLM analysis showed that quasi-horizontal transport is only weakly inhibited and results in inhomogeneous mixing of tropical and extratropical air masses. In these cases, correlations hint at the presence of a dynamical barrier to transport. A discontinuous jump in the correlation curve more clearly identifies that a strong barrier to mixing exists. Therefore, correlations can resolve transport issues but are more precisely interpreted when coupled with a NMLM analysis.

In conclusion, combining ER-2 tracer correlations with a HALOE NMLM analysis provides increased information for evaluating the role of transport in the lower stratosphere on both small and large scales. When tracer correlations and NMLM analyses are used in conjunction, one analysis can suggest and the other verify the role of transport. However, the NMLM technique is far preferred to tracer correlations if only one analysis is employed to deduce information about transport. This analysis not only captures the tracer distribution but also identifies the location, shape and relative strength of transport barriers and mixing regions. A weakness of the method is that it depends upon using global satellite data of lower resolution (compared to aircraft data). However, we were able to assess the satellite data by comparing tracer correlations based upon HALOE measurements with those from the ER-2. Correlations were examined for time periods that coincided with ER-2 flights from 1991 through 1997. Fortunately, the very good agreement achieved between the CH_4 versus O_3 correlations from the two independent sources increased our

confidence in using the HALOE CH₄ data in global NMLM analyses which provide a much more quantitative interpretation of the transport.

LIST OF REFERENCES

- Andrews, D. G., J. R. Holton, and C. B. Leovy, *Middle Atmosphere Dynamics*, 489 pp., Academic Press, Orlando, Fla., 1987.
- Boering, K. A., B. C. Daube, S. C. Wofsy, M. Loewenstein, J. R. Podolske, and E. R. Keim, Tracer-tracer relationships and lower stratospheric dynamics: CO₂ and N₂O correlations during SPADE, *Geophys. Res. Lett.*, *21*, 2567-2571, 1994.
- Brewer, A. W., Evidence for a world circulation provided by the measurements of helium and water vapor distribution in the stratosphere, *Q. J. R. Meteorol. Soc.*, *75*, 351-363, 1949.
- Bruhl, C., S. R. Drayson, J. M. Russell III, P. J. Crutzen, J. M. McInerney, P. N. Purcell, H. Claude, H. Gernandt, T. J. McGee, I. S. McDermid, and M. R. Gunson, Halogen Occultation Experiment ozone channel validation, *J. Geophys. Res.*, *101*, 10217-10240, 1996.
- Brasseur, G., and S. Solomon, *Aeronomy of the Middle Atmosphere*, 452 pp., D. Reidel, Norwell, Mass., 1986.
- Buchart, N., and E. E. Remsberg, The area of the stratospheric polar vortex as a diagnostic for tracer transport on an isentropic surface, *J. Atmos. Sci.*, *43*, 1319-1339, 1986.
- Chen, P., J. R. Holton, A. O'Neill, and R. Swinbank, Isentropic mass exchange between the tropics and extratropics in the stratosphere, *J. Atmos. Sci.*, *51*, 3006-3018, 1994.
- Collins, J. E., Jr., G. W. Sachse, B. E. Anderson, A. J. Weinheimer, J. G. Walega, and B. A. Ridley, AASE-II in-situ tracer correlations of methane, nitrous oxide, and ozone as observed aboard the DC-8, *Geophys. Res. Lett.*, *20*, 2543-2546, 1993.
- Dahlberg, S. P., and K. P. Bowman, Climatology of large-scale isentropic mixing in the Arctic winter stratosphere from analyzed winds, *J. Geophys. Res.*, *99*, 20585-20599, 1994.
- Dobson, G. M. B., Origin and distribution of the polyatomic molecules in the atmosphere, *Proc. R. Soc. London, Ser. A*, *236*, 187-193, 1956.

- Fahey, D. W., K. K. Kelly, S. R. Kawa, A. F. Tuck, M. Loewenstein, K. R. Chan, and L. E. Heidt, Observations of denitrification and dehydration in the winter polar stratosphere, *Nature*, 344, 321-324, 1990a.
- Fahey, D. W., S. Solomon, S. R. Kawa, M. Loewenstein, J. R. Podolske, S. E. Strahan, and K. R. Chan, A diagnostic for denitrification in the winter polar stratosphere, *Nature*, 345, 698-702, 1990b.
- Fairlie, T. D. A., Three-dimensional transport simulations of the dispersal of volcanic aerosol from Mount Pinatubo, M.S. thesis, 131 pp., Old Dominion Univ., August 1993.
- Farman, J. C., B. G. Gardiner, and J. D. Shanklin, Large losses of total ozone in Antarctica reveal seasonal ClO_x/NO_x interaction, *Nature*, 315, 207-210, 1985.
- Haltiner, G. S., and R. T. Williams, *Numerical Prediction and Dynamic Meteorology*, 477 pp., John Wiley & Sons, New York, 1980.
- Holton, J. R., A dynamical based transport parameterization for one-dimensional photochemical models of the stratosphere, *J. Geophys. Res.*, 91, 2681-2686, 1986a.
- Holton, J. R., Meridional distribution of stratospheric trace constituents, *J. Atmos. Sci.*, 43, 1238-1242, 1986b.
- Holton, J. R., *An Introduction to Dynamic Meteorology*, 511 pp., Academic Press, San Diego, Calif., 1992.
- Holton, J. R., P. H. Haynes, M. E. McIntyre, A. R. Douglass, R. B. Rood, and L. Pfister, Stratosphere-troposphere exchange, *Rev. Geophys.*, 33, 403-439, 1995.
- Jones, R. L., and J. A. Pyle, Observations of CH₄ and N₂O by the NIMBUS 7 SAMS: A comparison with in situ data and two-dimensional numerical model calculations, *J. Geophys. Res.*, 89, 5263-5279, 1984.
- Lahoz, W. A., A. O'Neill, A. Heaps, V. D. Pope, R. Swinbank, R. S. Harwood, L. Froidevaux, W. G. Reed, J. W. Waters, and G. E. Peckham, Vortex dynamics and the evolution of water vapor in the stratosphere of the southern hemisphere, *Q. J. R. Meteorol. Soc.*, 122, 423-450, 1995.
- Mahlman, J. D., H. Levy II, and W. J. Moxim, Three-dimensional simulations of stratospheric N₂O: Predictions for other trace constituents, *J. Geophys. Res.*, 91, 2687-2707, 1986.

- McIntyre, M. E., and T. N. Palmer, Breaking planetary waves in the stratosphere, *Nature*, 305, 593-600, 1983.
- Murphy, D. M., A. F. Tuck, K. K. Kelly, K. R. Chan, M. Loewenstein, J. R. Podolske, M. H. Proffitt, and S. E. Strahan, Indicators of transport and vertical motion from correlations between in situ measurements in the Airborne Antarctic Ozone Experiment, *J. Geophys. Res.*, 94, 11669-11685, 1989.
- Murphy, D. M., D. W. Fahey, M. H. Proffitt, S. C. Liu, K. R. Chan, C. S. Eubank, S. R. Kawa, and K. K. Kelly, Reactive nitrogen and its correlation with ozone in the lower stratosphere and upper troposphere, *J. Geophys. Res.*, 98, 8751-8773, 1993.
- Nakamura, N., Modified Lagrangian-mean diagnostics of the stratospheric polar vortices. Part 1: Formulation and analysis of GFDL SKYHI GCM, *J. Atmos. Sci.*, 52, 2096-2108, 1995.
- Nakamura, N., Two-dimensional mixing, edge formation, and permeability diagnosed in an area coordinate, *J. Atmos. Sci.* 53, 1524-1537, 1996.
- Nakamura, N., and J. Ma, Modified Lagrangian-mean diagnostics of the stratospheric polar vortices. Part 2: Nitrous oxide and seasonal barrier migration in the cryogenic limb array etalon spectrometer and SKYHI general circulation model, *J. Geophys. Res.*, 102, 25721-25735, 1997.
- Nakamura, N., Leaky containment vessels of air: A Lagrangian-mean approach to the stratospheric tracer transport, in *Advances in Fluid Mechanics: Dynamics of Atmospheric Flows, part I, Atmospheric Transport and Diffusion Processes*, edited by M. P. Singh and S. Raman, pp. 193-246, Comput. Mech. Publ., Ashurst, England, 1998.
- Nakamura, N., J. Ma, and J. J. Modi, Deciphering Lagrangian-mean transport and chemistry from the stratospheric trace constituents data, in *Recent Advances in Stratospheric Processes*, edited by T. Nathan and E. Cordero, pp. 46-76, Research Signpost, Trivandurm, India, 1999.
- O'Sullivan, D., and T. J. Dunkerton, The influence of the quasi-biennial oscillation on global constituent distributions, *J. Geophys. Res.*, 102, 21731-21743, 1997.
- Park, J. H., J. M. Russell III, L. L. Gordley, S. R. Drayson, D. C. Benner, J. M. McInerney, M. R. Gunson, G. C. Toon, B. Sen, J.-F. Blavier, C. R. Webster, E. C. Zipf, P. Erdman, U. Schmidt, and C. Schiller, Validation of Halogen Occultation Experiment CH₄ measurements from the UARS, *J. Geophys. Res.*, 101, 10183-10203, 1996.

- Pierce, R. B., and T. D. A. Fairlie, Chaotic advection in the stratosphere: Implications for the dispersal of chemically perturbed air from the polar vortex, *J. Geophys. Res.*, *98*, 18589-18595, 1993.
- Pierce, R. B., T. D. Fairlie, E. E. Remsberg, J. M. Russell III, and W. L. Grose, HALOE observations of the Arctic vortex during the 1997 spring: Horizontal structure in the lower stratosphere, *Geophys. Res. Lett.*, *24*, 2701-2704, 1997.
- Plumb, R. A., and M. K. W. Ko, Interrelationships between mixing ratios of long-lived stratospheric constituents, *J. Geophys. Res.*, *97*, 10145-10156, 1992.
- Plumb, R. A., D. W. Waugh, R. J. Atkinson, P. A. Newman, L. R. Lait, M. R. Schoeberl, E. V. Browell, A. J. Simmons, and M. Loewenstein, Intrusions into the lower stratospheric Arctic vortex during the winter of 1991-1992, *J. Geophys. Res.*, *99*, 1089-1105, 1994.
- Plumb, R. A., A "tropical pipe" model of stratospheric transport, *J. Geophys. Res.*, *101*, 3957-3972, 1996.
- Proffitt, M. H., and R. J. McLaughlin, Fast-response dual-beam UV-absorption ozone photometer suitable for use on stratospheric balloons, *Rev. Sci. Instrum.*, *54*, 1719-1728, 1983.
- Proffitt, M. H., D.W. Fahey, K.K. Kelly, and A.F. Tuck, High-latitude ozone loss outside the Antarctic ozone hole, *Nature*, *342*, 233-237, 1989a.
- Proffitt, M. H., M. J. Steinkamp, J. A. Powell, R. J. McLaughlin, O. A. Mills, A. L. Schmeltekopf, T. L. Thompson, A. F. Tuck, T. Tyler, R. H. Winkler, and K. R. Chan, In situ ozone measurements within the 1987 Antarctic ozone hole from a high-altitude ER-2 aircraft, *J. Geophys. Res.*, *94*, 16,547-16,555, 1989b.
- Proffitt, M. H., J. J. Margitan, K. K. Kelly, M. Loewenstein, J. R. Podolske, and K. R. Chan, Ozone loss in the Arctic polar vortex inferred from high-altitude aircraft measurements, *Nature*, *342*, 31-36, 1990.
- Reber, C. A., The Upper Atmosphere Research Satellite (UARS), *Geophys. Res. Lett.*, *20*, 1215-1218, 1993.
- Remsberg, E. E., and P. P. Bhatt, Zonal variance of nitric acid vapor as an indicator of meridional mixing in the subtropical lower stratosphere, *J. Geophys. Res.*, *101*, 29523-29530, 1996.

- Roche, A. E., J. B. Kummer, J. L. Mergenthaler, G. A. Ely, W. G. Uplinger, J. F. Potter, T. C. James, and L. W. Sterritt, The Cryogenic Limb Array Etalon Spectrometer (CLAES) on UARS: Experiment description and performance, *J. Geophys. Res.*, *98*, 10763-10775, 1993.
- Roche, A. E., J. B. Kummer, R. W. Nightingale, J. L. Mergenthaler, G. A. Ely, P. L. Bailey, S. T. Massie, J. C. Gille, D. P. Edwards, M. R. Gunson, M. C. Abrams, G. C. Toon, C. R. Webster, W. A. Traub, K. W. Jucks, D. G. Johnson, D. G. Murcray, F. H. Murcray, A. Goldman, and E. C. Zipf, Validation of CH₄ and N₂O measurements by the cryogenic limb array etalon spectrometer instrument on the Upper Atmosphere Research Satellite, *J. Geophys. Res.*, *101*, 9679-9710, 1996.
- Russell, J. M., III, L. L. Gordley, J. H. Park, S. R. Drayson, W. D. Hesketh, R. J. Cicerone, A. F. Tuck, J. E. Frederick, J. E. Harries, and P. J. Crutzen, The Halogen Occultation Experiment, *J. Geophys. Res.*, *98*, 10,777-10,797, 1993.
- Ruth, S. L., J. J. Remedios, B. N. Lawrence, and F. W. Taylor, Measurements of N₂O by the UARS Improved Stratospheric and Mesospheric Sounder during the early northern winter 1991/92, *J. Atmos. Sci.*, *51*, 2818-2833, 1994.
- Ruth, S., R. Kennaugh, L. J. Gray, and J. M. Russell III, Seasonal, semiannual, and interannual variability seen in measurements of methane made by the UARS Halogen Occultation Experiment, *J. Geophys. Res.*, *102*, 16189-16199, 1997.
- Salawitch, R. J., et al., The distribution of hydrogen, nitrogen, and chlorine radicals in the lower stratosphere: Implications for changes in O₃ due to emission of NO_y from supersonic aircraft, *Geophys. Res. Lett.*, *21*, 2547-2550, 1994a.
- Salawitch, R. J., et al., The diurnal variation of hydrogen, nitrogen, and chlorine radicals: Implications for the heterogeneous production of HNO₂, *Geophys. Res. Lett.*, *21*, 2551-2554, 1994b.
- Salby, M. L., and R. R. Garcia, Dynamical perturbations of the ozone layer, *Physics Today*, *43*, 38-46, 1990.
- Schoeberl, M. R., L. R. Lait, P. A. Newman, and J. E. Rosenfield, The structure of the polar vortex, *J. Geophys. Res.*, *97*, 7859-7882, 1992.
- Swinbank, R., and A. O'Neill, A stratosphere-troposphere assimilation system, *Mon. Wea. Rev.*, *122*, 686-702, 1994.
- Trepte, C. R., and M. H. Hitchman, Tropical stratospheric circulation deduced from satellite aerosol data, *Nature*, *355*, 626-628, 1992.

- Volk, C. M., J. W. Elkins, D. W. Fahey, R. J. Salawitch, G. S. Dutton, J. M. Gilligan, M. H. Proffitt, M. Loewenstein, J. R. Podolske, K. Minschwaner, J. J. Margitan, and K. R. Chan, Quantifying transport between the tropical and mid-latitude lower stratosphere, *Science*, 272, 1763-1768, 1996.
- Waugh, D. W., Seasonal variation of isentropic transport out of the tropical stratosphere, *J. Geophys. Res.*, 101, 4007-4023, 1996.
- Waugh, D. W., R. A. Plumb, J. W. Elkins, D. W. Fahey, K. A. Boering, G. S. Dutton, C. M. Volk, E. Keim, R.-S. Gao, B. C. Daube, S. C. Wofsy, M. Loewenstein, J. R. Podolske, K. R. Chan, M. H. Proffitt, K. K. Kelly, P. A. Newman, and L. R. Lait, Mixing of polar vortex air into middle latitudes as revealed by tracer-tracer scatterplots, *J. Geophys. Res.*, 102, 13119-13134, 1997.
- Webster, C. R., R. D. May, C. A. Trimble, R. G. Chave, and J. Kendall, Aircraft (ER-2) Laser Infrared Absorption Spectrometer (ALIAS) for in situ stratospheric measurements of HCl, N₂O, CH₄, NO₂, and HNO₃, *Appl. Opt.*, 33, 454-472, 1994.
- World Meteorological Organization, Scientific Assessment of Ozone Depletion: 1998, *WMO-Global Ozone Research and Monitoring Project Rep. 44*, 605 pp., 1999.

VITA

Gretchen Scott Lingenfelter

Gretchen Scott Lingenfelter was born in Newport News, Virginia on April 20, 1951. She graduated from Kecoughtan High School in Hampton, Virginia in June 1969. In February of 1970, she began her 30 year career as a government contractor supporting the National Aeronautics and Space Administration (NASA) at Langley Research Center (LaRC) in Hampton. While employed with the General Electric Company (1970-1976) and Analytical Mechanics Associates Incorporated (1977-1988), she attended Christopher Newport College in Newport News and received the Bachelor of Science degree in Mathematics, graduating cum laude and with a Superior Achievement in Mathematics award, in August 1987.

From 1988 to 1992, she held the position of Senior Scientist with Hughes STX Corporation at LaRC where she was active in atmospheric science research. From 1992 to the present, she has held the position of Atmospheric Scientist with Science Applications International Corporation, also at LaRC. Her responsibilities include assessment and interpretation of data from satellite-borne sensors, from internally generated atmospheric simulation models, and from aircraft in situ measurements to study the chemical, dynamical, and radiative processes of the Earth's stratosphere.

In the fall of 1993, the author was admitted to the College of William and Mary in the Masters Program in Applied Science.